Sequence Variation in Hepatitis C Virus Nonstructural Protein 5A Predicts Clinical Outcome of Pegylated Interferon/Ribavirin Combination Therapy

Ahmed El-Shamy,[1] Motoko Nagano-Fujii,[1] Noriko Sasase,[2] Susumu Imoto,[2] Soo-Ryang Kim,[2] and Hak Hotta[1,3]

A substantial proportion of hepatitis C virus (HCV)-1b–infected patients still do not respond to interferon-based therapy. This study aims to explore a predictive marker for the ultimate virological response of HCV-1b–infected patients treated with pegylated interferon/ribavirin (PEG-IFN/RBV) combination therapy. Nonstructural protein 5A (NS5A) sequences of HCV in the pretreated sera of 45 patients infected with HCV-1b were analyzed. The mean number of mutations in the variable region 3 (V3) plus its upstream flanking region of NS5A (amino acid 2334-2379), referred to as IFN/RBV resistance-determining region (IRRDR), was significantly higher for HCV isolates obtained from patients who later achieved sustained virological response (SVR) by PEG-IFN/RBV than for those in patients undergoing non-SVR. The receiver operating characteristic curve analysis estimated six mutations in IRRDR as the optimal threshold for SVR prediction. Indeed, 16 (76%) of 21 SVR, but only 2 (8%) of 24 non-SVR, had HCV with six or more mutations in IRRDR (IRRDR ≥ 6) ($P < 0.0001$). All of 18 patients infected with HCV of IRRDR of 6 or greater examined showed a significant (≥1 log) reduction or disappearance of serum HCV core antigen titers within 24 hours after initial dose of PEG-IFN/RBV, whereas 10 (37%) of 27 patients with HCV of IRRDR of 5 or less did ($P < 0.0001$). The positive predictive value of IRRDR of 6 or greater for SVR was 89% (16/18; $P = 0.0007$), with its negative predictive value for non-SVR being 81% (22/27; $P = 0.0008$). *Conclusion:* A high degree (≥6) of sequence variation in IRRDR would be a useful marker for predicting SVR, whereas a less diverse (≤5) IRRDR sequence predicts non-SVR. (HEPATOLOGY 2008;48:38-47.)

Hepatitis C virus (HCV) infection is the major cause of chronic hepatitis, liver cirrhosis, and hepatocellular carcinoma in industrialized countries. However, HCV infection is curable, and its complications can be prevented by antiviral therapy.[1,2] Currently, the most effective treatment of chronic HCV infection is based on a combination of pegylated interferon (PEG-IFN) and ribavirin (RBV).[3] Even with this treatment regimen, however, sustained virological response (SVR) rates for those infected with the most resistant genotypes, HCV-1a and HCV-1b, still hover at approximately 50%.[3,4] Considering the high cost and the significant side effects associated with this combination therapy, it is worthy to identify patients most likely to benefit from therapy.[5] Predictors of IFN-based therapy can be classified into two categories, pretreatment and on-treatment factors. Pretreatment factors comprise host factors, such as age, sex, obesity, ethanol consumption, hepatic iron overload, fibrosis, immune responses, and coinfection with other viruses, and viral factors, which mainly include viral genotypes and viral load. On-treatment factors are mainly related to the viral kinetics within

Abbreviations: aa, amino acid; CI, confidence interval; CNR, complete nonresponse; ETR, end-of-treatment response; EVR, early virological response; HCV, hepatitis C virus; IFN, interferon; IRRDR, interferon/ribavirin resistance-determining region; ISDR, interferon sensitivity-determining region; NS5A, nonstructural protein 5A; nt, nucleotide; PEG, pegylated; PKR-BD, double-stranded RNA-activated protein kinase-binding domain; RBV, ribavirin; RT-PCR, reverse transcription polymerase chain reaction; SVR, sustained virological response; V3, variable 3.

From the [1]Division of Microbiology, Kobe University Graduate School of Medicine, Kobe, Japan; [2]Division of Gastroenterology, Kobe Asahi Hospital, Kobe, Japan; and [3]International Center for Medical Research and Treatment, Kobe University Graduate School of Medicine, Kobe, Japan.

Received August 10, 2007; accepted March 11, 2008.

Supported in part by grants-in-aid for scientific research from the Ministry of Education, Culture, Sports, Science, and Technology and the Ministry of Health, Labour, and Welfare of Japan. This study was also carried out as part of the Program of Founding Research Centers for Emerging and Reemerging Infectious Diseases (Ministry of Education, Culture, Sports, Science and Technology) and the 21st Century Center of Excellence program at Kobe University Graduate School of Medicine.

Address reprint requests to: Hak Hotta, M.D., Ph.D., Division of Microbiology, Kobe University Graduate School of Medicine, 7-5-1 Kusunoki-cho, Chuo-ku, Kobe 650-0017, Japan. E-mail: hotta@kobe-u.ac.jp; fax: (81)-78-382-5519.

Published online in Wiley InterScience (www.interscience.wiley.com).

DOI 10.1002/hep.22339

Potential conflict of interest: Nothing to report.

the first few weeks of treatment.[6] Because the HCV genotype is one of the major factors affecting IFN-based therapy response, IFN resistance is, at least partly, genetically encoded by HCV itself.[7] In this context, nonstructural protein 5A (NS5A), one of the HCV nonstructural proteins, has been widely discussed for its correlation with IFN responsiveness. Enomoto et al.[8,9] proposed that the sequence variations within a region in NS5A, called the IFN sensitivity-determining region (ISDR), is correlated with IFN responsiveness. It was further demonstrated that ISDR and its adjacent sequence was able to bind to double-stranded RNA-activated protein kinase (PKR), one of the important antiviral proteins of the host cell, to inhibit its enzymatic activity and, therefore, the combined region is called PKR-binding domain (PKR-BD).[10,11] A significant correlation between sequence variation in PKR-BD and IFN responsiveness was also reported.[12] In addition, there are some reports that showed a correlation between IFN responsiveness and the sequence diversity of the variable region 3 (V3) [amino acids (aa) 2356 to 2379] or its surrounding regions near the carboxy terminus of NS5A.[12-20]

We have recently reported that a high degree of sequence variations in the V3 and the pre-V3 regions (aa 2334-2355) of NS5A, which we collectively refer to as IFN/RBV resistance-determining region (IRRDR) (aa 2334-2379), was closely correlated with early virological response (EVR) by week 16 in HCV-1b–infected patients treated with PEG-IFN and RBV.[21] In the current study, we aimed to follow up our previous observations to investigate whether the degree of sequence variation in IRRDR could also correlate with SVR on PEG-IFN/RBV combination therapy.

Patients and Methods

Patients. A total of 45 patients chronically infected with HCV-1b, whose diagnoses had been made based on anti-HCV antibody detection, HCV subtype determination according to the method by Okamoto et al.,[22] and clinical follow-up, were treated with PEG-IFN α-2b (1.5 μg/kg body weight, once weekly, subcutaneously) and RBV (600-800 mg daily, per os), according to a standard treatment protocol for Japanese patients established by a hepatitis study group of the Ministry of Health, Labour, and Welfare, Japan, at Kobe Asahi Hospital, Hyogo Prefecture, Japan. All the patients were confirmed negative for hepatitis B surface antigen using chemiluminescent immunoassay (Abbott Japan Co., Ltd., Tokyo, Japan). Serum samples were collected from the patients at intervals of 4 weeks before, during, and after the treatment, and tested for HCV RNA by reverse transcription polymerase chain reaction (RT-PCR), as reported previously.[21] The quantification of serum HCV RNA titers was performed by RT-PCR with an internal RNA standard derived from the 5′ noncoding region of HCV (Amplicor HCV Monitor test, version 2.0, Roche Diagnostics, Tokyo, Japan). The thresholds of the low-range and high-range measurements of this assay were 50 and 600 IU/mL, respectively. HCV core antigen in the sera was also quantitatively measured by chemiluminescent immunoassay (Abbott Japan Co., Ltd., Tokyo, Japan). The threshold of this assay is 20 fmol/L.

The study protocol was approved beforehand by the Ethic Committee in Kobe Asahi Hospital, and written informed consent was obtained from each patient before the treatment.

NS5A Sequence Analysis. HCV RNA was extracted from 140 μL serum using a commercially available kit (QIAmp viral RNA kit; QIAGEN, Tokyo, Japan). For amplification of the NS5A region of the HCV genome, the extracted RNA was reverse transcribed and amplified for full-length NS5A using SuperScript One-step RT-PCR for long templates (Invitrogen, Tokyo, Japan) and a set of primers, NS5A-F1 [5′-TACTCCCTGCCATCCTCTCTCCTG-3′; sense, nucleotides (nt) 5974-5997] and NS5A-F2 (5′-CTCCTTGAGCACGTCCCGGT-3′; antisense, nt 7777-7796). The resultant RT-PCR product was subjected to a second-round PCR by using Platinum Taq DNA polymerase (Invitrogen) and an inner set of primers, NS5A-F3 (5′TCTCCAGCCTTACCATCACYCA-3′; sense, nt 6172-6193) and NS5A-F4 (5′-CGGTARTGRTCGTCCAGGAC-3′; antisense, nt 7761-7780). The samples that were not amplifiable (nos. 3, 23, 47, 61, 65, and 69) using the aforementioned primers were amplified using primer sets reported previously.[23] Reverse transcription was performed at 45°C for 30 minutes and terminated at 94°C for 2 minutes, followed by the first-round PCR over 35 cycles, with each cycle consisting of denaturation at 94°C for 30 seconds, annealing at 55°C for 30 seconds and extension at 68°C for 90 seconds. The second-round PCR was performed under the same condition. The amplified fragments were purified with QIA quick PCR purification kit (QIAGEN), and visualized by agarose gel electrophoresis and ethidium bromide staining. The sequences of the amplified fragments were determined by direct sequencing without subcloning using Big Dye Deoxy Terminator cycle sequencing kit and ABI 337 DNA sequencer (Applied Biosystems, Inc, Japan). The aa sequences were deduced and aligned using GENETYX Win software version.7.0 (GENETYX Corp., Tokyo, Japan). Numbering of aa throughout the complete manuscript is according to the poly protein of HCV genotype 1b prototype HCV-J.[24]

Statistical Analysis. Statistical difference in the parameters, including all available patients' demographic, biochemical, hematological, and virological data as well as IRRDR sequence variations factors, was determined between different patients' groups by Student t test for numerical variables, and Fisher's exact probability test for categorical variables. In the case of multiple comparisons for various regions of NS5A, P values were adjusted by the Bonferroni method to reduce the probability of erroneously classifying nonsignificant hypothesis as significant. Although there are five regions of comparison (full-NS5A, N-half, ISDR, PKR-BD and IRRDR), the ISDR is entirely within the PKR-BD, and all the regions fall within the full-NS5A. Therefore, it would be reasonable to adjust the P values for three regions of comparison. Accordingly, the P value for a test was multiplied by 3. To evaluate the optimal threshold of IRRDR mutations for SVR prediction, the receiver operating characteristic curve was constructed and the area under the curve as well as the sensitivity and specificity were calculated. Subsequently, univariate and multivariate logistic analyses were performed to identify variables that independently predict SVR. The odds ratios and 95% confidence intervals (95% CI) were also calculated. Kaplan-Meier HCV survival curve analysis was performed based on serum HCV-RNA positivity data during treatment period (48 weeks) according to the number of IRRDR mutations (IRRDR $\geq$ 6 and IRRDR $\leq$ 5). The HCV death event was estimated as the first time point of HCV-RNA clearance after initiation of the treatment. The data obtained were evaluated by the log-rank test. Positive and negative predictive values of SVR predictors were computed, and their significance levels were evaluated using the sign test. All statistical analyses were performed using the SPSS version 16 software (SPSS Inc., Chicago, IL). Unless otherwise stated, a P value of less than 0.05 was considered statistically significant.

Nucleotide Sequence Accession Numbers. The sequence data reported in this article have been deposited in the DDBJ/EMBL/GenBank nucleotide sequence databases with the accession numbers AB285035 through AB285081, and AB354116 through AB354118.

Results

Virological Responses of the Patients Treated with PEG-IFN and RBV. Proportions of various virological responses of the patients treated with PEG-IFN/RBV combination therapy are shown in Table 1. Of 45 patients enrolled in this study, 23 (51%), 31 (69%), and 21 (47%) patients, respectively, achieved EVR by week 12 [EVR(12w)], end-of-treatment response (ETR), and sustained virological response (SVR). Among 23 patients with EVR(12w), 22 (96%) and 18 patients (78%) achieved ETR and SVR, respectively. This indicates that EVR(12w) was significantly correlated with ETR and SVR ($P < 0.0001$). A total of 24 patients (53%) failed to achieve SVR, and they were referred to as non-SVR. Non-SVR can be divided into two categories: (i) complete nonresponse (CNR), which is defined by continued presence of serum HCV RNA up to the end of the treatment, and (ii) relapse, which is defined by transient disappearance of HCV RNA at a certain time point followed by reappearance of HCV RNA either before or after the end of the treatment. CNR represented 24% (11/45) of all cases and 46% (11/24) of non-SVR. Thirteen (29%) of 45 patients underwent relapse. Among 13 relapsers, 3 (23%) patients had rebound in HCV viremia before the end of the treatment and, hence, were defined as undergoing viral breakthrough, whereas 10 (77%) patients had rebound in HCV viremia after the end of the treatment, defined as ETR-relapsers.

Table 1. Proportions of Various Virological Responses of Patients Treated With PEG-IFN/RBV

Virological Response	Proportion
EVR(12w)	51% (23/45)*
ETR	69% (31/45)
SVR	47% (21/45)
Non-SVR	53% (24/45)
CNR	24% (11/45)
Relapse	29% (13/45)
ETR-relapse	22% (10/45)
Viral breakthrough	7% (3/45)

*No. of patients/no. of total.

Abbreviations: PEG-IFN/RBV, pegylated-interferon/ribavirin; EVR, early virological response; ETR, end-of-treatment response; SVR, sustained virological response; CNR, complete nonresponse.

Demographic characteristics of patients with SVR, non-SVR, CNR, and relapse are summarized in Table 2. Age, sex, body weight, hemoglobin levels, or gamma guanosine triphosphate titers did not significantly differ between SVR and non-SVR or CNR. However, patients with SVR showed a trend toward having significantly higher platelet counts than those with non-SVR and CNR. Also, the mean initial titers of HCV core antigen for non-SVR and CNR, respectively, were 1.6 times and 2.3 times higher than that for SVR, although the difference was not statistically significant. HCV RNA titers were almost the same among them.

Correlation Between Virological Responses and the Sequence Variation of IRRDR of HCV NS5A Obtained from the Pretreated Sera. The entire NS5A region of the HCV genome was amplified from the pretreated sera and the aa sequences deduced. We compared

Table 2. Demographic Characteristics of Patients With SVR, Non-SVR, CNR, and Relapse

Factor	SVR	Non-SVR	CNR	Relapse	*P* Value		
					SVR versus Non-SVR	SVR versus CNR	SVR versus Relapse
Age	56.5 ± 8.0*	59.9 ± 10.6	59.4 ± 10.0	60.3 ± 11.5	NS†	NS	NS
Sex (male/female)	12/9	13/11	6/5	7/6	NS	NS	NS
Body weight (kg)	58.5 ± 9.4	59 ± 13.2	61.0 ± 10.8	57.8 ± 15.3	NS	NS	NS
Platelets ($\times 10^4/mm^3$)	18.3 ± 4.4	15.0 ± 4.9	12.3 ± 3.9	16.8 ± 4.9	0.02‡	0.001‡	NS
Hemoglobin (g/dL)	14.1 ± 1.3	13.7 ± 1.4	14.4 ± 1.3	14.3 ± 1.5	NS	NS	NS
γ-GTP (IU/L)	43.5 ± 28.7	51.6 ± 35.7	62.8 ± 40.3	43.8 ± 30.5	NS	NS	NS
HCV-RNA (KIU/mL)	1326 ± 1256	1667 ± 1311	1488 ± 1228	1818 ± 1408	NS	NS	NS
HCV core antigen (fmol/L)	6183 ± 6894	9830 ± 1214	14,033 ± 17,089	6481 ± 4023	NS	NS	NS

*Mean ± SD.
†Not significant.
‡Student *t* test.
Abbreviations: SVR, sustained virological response; CNR, complete nonresponse; γ-GTP, gamma guanosine triphosphate.

each NS5A sequence with a consensus sequence inferred from aligning the previously published NS5A-1b sequences.[8] In this connection, the consensus sequence for IRRDR differs from the corresponding sequence of a prototype strain of IFN resistance HCV-1b (HCV-J; DDBJ/EMBL/Genbank accession no. D90208) by a single residue at position 2367 (Ala instead of Gly). Because Ala^{2367} was conserved in 95% of the reported sequences, we used the IRRDR consensus sequence in this study. As shown in Table 3, the mean number of aa substitutions in the entire NS5A obtained from patients with SVR was significantly greater compared with non-SVR and relapse. There was no difference in the number of mutations in an N-terminal half of NS5A (aa 1972-2208), the ISDR (aa 2209-2248) or the PKR-BD (aa 2209-2274) between the different patients' groups. Conversely, we found a more obvious significant difference in the mean numbers of aa mutations within a region consisting of the pre-V3 and V3 regions, which we refer to as IRRDR, between SVR and other patients' groups (Table 3).

To estimate a cutoff number of mutations in IRRDR predicting SVR, the receiver operating characteristics analysis was performed. The result revealed that six mutations were an optimal number of mutations to predict SVR, because it achieved the highest sensitivity (76%) combined with the highest specificity (92%) and yielded an area under the curve of 0.81 (Fig. 1).

Indeed, only 2 (8%) of 24 patients with non-SVR, in contrast to 16 (76%) of 21 patients with SVR, had HCV with IRRDR of 6 or greater, with the difference between the two groups being statistically significant ($P < 0.0001$) (Table 4). Furthermore, none of 11 patients with CNR had HCV of IRRDR of 6 or greater, and the difference between SVR and CNR was statistically significant ($P < 0.0001$). Similarly, only 2 (15%) of 13 relapsers (10 ETR-relapsers + 3 patients with viral breakthrough) had HCV of IRRDR greater than or equal to 6, with the result demonstrating significant difference between SVR and relapse ($P = 0.001$).

Table 3. Average Numbers of aa Mutations Within Different Regions of HCV NS5A Obtained From Pretreated Sera of Patients With SVR, Non-SVR, CNR, and Relapse

NS5A Region	No. of Mutations*				*P* Value†		
	SVR	Non-SVR	CNR	Relapse	SVR versus Non-SVR	SVR versus CNR	SVR versus Relapse
Full-NS5A (aa 1972-2419)	24.9 ± 6.1*	19.7 ± 4.3	20.1 ± 5.2	19.4 ± 3.5	0.012	0.144	0.03
N-half (aa 1972-2208)	9.2 ± 1.9	8.6 ± 1.9	9.0 ± 2.4	8.2 ± 1.2	NS‡	NS	NS
ISDR (aa 2209-2248)	2.1 ± 2.8	1.2 ± 1.1	1.7 ± 1.4	0.8 ± 0.7	NS	NS	NS
PKR-BD (aa 2209-2274)	3.8 ± 3.4	2.5 ± 2.0	2.9 ± 2.4	2.1 ± 1.5	NS	NS	NS
IRRDR (aa 2334-2379)	6.1 ± 2.1	3.9 ± 1.4	3.7 ± 0.9	4.0 ± 1.8	0.0006	0.003	0.018

*Mean ± SD.
†The *P* values obtained with Student *t* test were adjusted using the Bonferroni method (see Materials and Methods).
‡Not significant.
Abbreviations: SVR, sustained virological response; CNR, complete nonresponse; aa, amino acid; ISDR: interferon sensitivity-determining region; PKR-BD, double-stranded RNA-activated protein kinase-binding domain; IRRDR, interferon/ribavirin resistance-determining region.

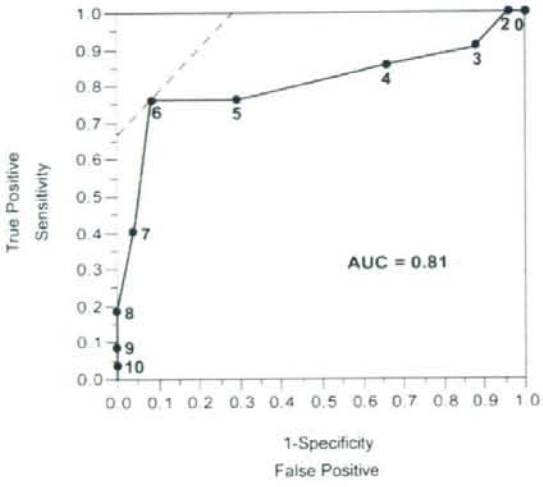

Fig. 1. The receiver operating characteristic curve analysis of IRRDR sequence variation for SVR prediction. The curve depicted with solid line shows an area under the curve of 0.81. Solid circles with numerals plotted on the curve represent different numbers of IRRDR mutations analyzed. The dashed line in the upper left corner indicates the optimal number of IRRDR mutations for SVR prediction, which yields the highest sensitivity (76%) and the highest specificity (92%).

When the IRRDR sequences obtained from all 45 patients were aligned along with the consensus sequence (Fig. 2), we noticed that 10 (48%) of 21 patients with SVR had alanine at position 2360 (Ala^{2360}), whereas only 3 (13%) of 24 patients with non-SVR and none of 11 patients with CNR did ($P = 0.02$ and 0.006, respectively) (Table 4). Similarly, 9 (43%) of 21 patients with SVR had threonine at position 2378 (Thr^{2378}), whereas only 3 (13%) of 24 patients with non-SVR and none of 11 patients with CNR did ($P = 0.04$ and 0.01, respectively).

To identify significant independent SVR predictors, we first entered all available baseline patients' features and IRRDR sequence variations data in univariate logistic analysis. As had been expected, this analysis yielded four factors significantly associated with SVR: IRRDR mutations, either continuous variable ($P < 0.0001$) or dichotomized at 6 ($P < 0.0001$), Ala^{2360} ($P = 0.002$), Thr^{2378} ($P = 0.019$), and platelet count ($P = 0.017$). Subsequently, we analyzed these four factors by multivariate logistic analysis. When the IRRDR mutations were dichotomized at 6, the multivariate analysis identified only the IRRDR of 6 or greater criterion as the independent predictor of SVR (odds ratio = 16.0; CI, 2.4-104.3; $P = 0.004$) (Table 5). However, when the IRRDR mutations were analyzed as a continuous variable, the multivariate analysis yielded IRRDR mutations (odds ratio = 1.8; CI, 1.1-3.1; $P = 0.02$) and Ala^{2360} (odds ratio = 9.3; CI, 1.1-78.8; $P = 0.04$) as independent SVR predictors.

Figure 3A shows the viral clearance rates of patients infected with HCV of IRRDR of 6 or greater and those with IRRDR of 5 or less at 4-week intervals during the whole observation period (72 weeks). All of 18 patients infected with HCV of IRRDR 6 or greater cleared the virus by week 16 and remained free of viremia thereafter until the end of the PEG-IFN/RBV treatment (week 48). Within 4 weeks after the cessation of the combination therapy, however, 2 (11%) of the 18 patients underwent relapse (ETR relapse). Conversely, 16 (59%) of the 27 patients with HCV of IRRDR of 5 or less cleared the virus by week 32. Of the 16 patients who once cleared the virus, 3 (19%) and 8 (50%) underwent relapse to become viral breakthrough and ETR relapsers, respectively.

Kaplan-Meier HCV survival curve analysis confirmed that, after the initiation of the IFN/RBV treatment, HCV clearance was achieved significantly more rapidly in patients infected with HCV isolates with IRRDR of 6 or greater than those with IRRDR of 5 or less, with the difference between the two groups being statistically significant ($P < 0.0001$) (Fig. 3B).

Sequence Analysis of ISDR and PKR-BD of HCV NS5A Obtained from Pretreated Sera. As described, there was no difference in the mean number of mutations in ISDR or PKR-BD between SVR and non-SVR or CNR (Table 3). Only four patients had HCV with four or

Table 4. Correlation Between NS5A Sequence Variation and Virological Responses of the Patients

	No. of Subjects / no. of Total*				P Value†		
Criteria	SVR	Non-SVR	CNR	Relapse	SVR versus Non-SVR	SVR versus CNR	SVR versus Relapse
IRRDR ≥ 6	16/21 (76%)	2/24 (8%)	0/11 (0%)	2/13 (15%)	< 0.0001	< 0.0001	0.001
Ala^{2360}	10/21 (48%)	3/24 (13%)	0/11 (0%)	3/13 (23%)	0.02	0.006	NS‡
Thr^{2378}	9/21 (43%)	3/24 (13%)	0/11 (0%)	3/13 (23%)	0.04	0.01	NS

*Total no. of SVR, Non-SVR, CNR, or relapse.

†Fisher's exact test.

‡Not significant.

Abbreviations: SVR, sustained virological response; CNR, complete nonresponse; IRRDR, interferon/ribavirin resistance-determining region; Ala^{2360}, alanine at position 2360; Thr^{2378}, threonine at position 2378.

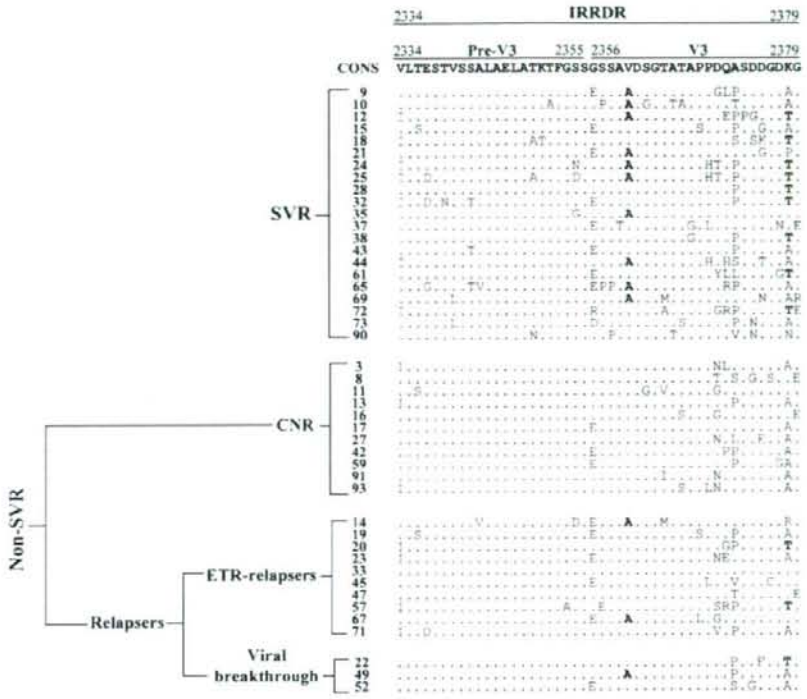

Fig. 2. Sequence alignment of IRRDR (Pre-V3 plus V3 regions) of NS5A of HCV-1b obtained from the pretreatment sera. The consensus sequence (Cons) is shown on the top. The Cons sequence differs from a prototype sequence of IFN-resistant HCV-1b (HCV-J; DDBJ/EMBL/GenBank accession no. D90208) by a single residue at position 2367 (alanine instead of glycine). The numbers along the sequence indicate aa positions. Dots indicate residues identical to those of the Cons sequence. Ala^{2360} and Thr^{2378} are written in boldface.

more mutations in ISDR (data not shown), the criterion for IFN-sensitive HCV strains according to Enomoto et al.[8,9] Although there appeared to be a trend for patients with HCV having four or more mutations in ISDR toward SVR (3 of 4), the difference was not statistically significant. Also, the prevalence of HCV with four or more mutations in ISDR was not significantly different between SVR (3 of 21; 14.3%) and non-SVR (1 of 24; 4.2%). It would be interesting to note, however, that all three HCV strains with four or more mutations in ISDR obtained from SVR (nos. 10, 65, and 72) had HCV of IRRDR of 6 or greater, whereas the only one strain with four or more mutations in ISDR from non-SVR (no. 13) had three mutations in IRRDR (data not shown). It is thus possible that the IRRDR sequence variation is associated with PEG-IFN/RBV responsiveness more closely than is the ISDR variation.

Table 5. Multivariate Logistic Regression Analysis to Identify Independent SVR Predictors

Factor	Odds (95% CI)	*P* value
Multivariate analysis 1		
IRRDR ≥ 6	16.0 (2.4-104.3)	0.004
Ala^{2360}	7.1 (0.8-66.8)	0.09
Thr^{2378}	4.1 (0.5-30.9)	0.17
Platelets	1.1 (0.9-1.4)	0.27
Multivariate analysis 2		
IRRDR mutations as a continuous variable	1.8 (1.1-3.1)	0.02
Ala^{2360}	9.3 (1.1-78.8)	0.04
Thr^{2378}	4.9 (0.7-33.3)	0.1
Platelets	1.2 (1.0-1.5)	0.08

Only factors that were significantly associated with SVR in univariate analysis were included in multivariate logistic regression analysis.

Abbreviations: IRRDR, interferon/ribavirin resistance-determining region; Ala^{2360}, alanine at position 2360; Thr^{2378}, threonine at position 2378; CI: confidence interval.

Correlation Between Rapid Reduction of HCV Core Antigen Titers and the Sequence Variation in IRRDR of HCV NS5A Obtained from the Pretreated Sera. As stated before, there was no significant difference in the mean values of initial HCV core antigen titers between patients with SVR and those with non-SVR (Table 2). However, we observed a strong association of SVR with rapid reduction of HCV core antigen titers during the very early stages of treatment, that is, 24 hours and 1, 2, and 4 weeks after the initiation of treatment (data not shown). Therefore, we analyzed whether the degree of sequence variation in IRRDR correlated with the very rapid reduction (24 hours after the first dose of PEG-IFN/RBV) of HCV core antigen titers. The result obtained clearly demonstrated a significant correlation between IRRDR of 6 or greater and the very rapid reduction of HCV core antigen titers 24 hours and 1, 2, and 4 weeks

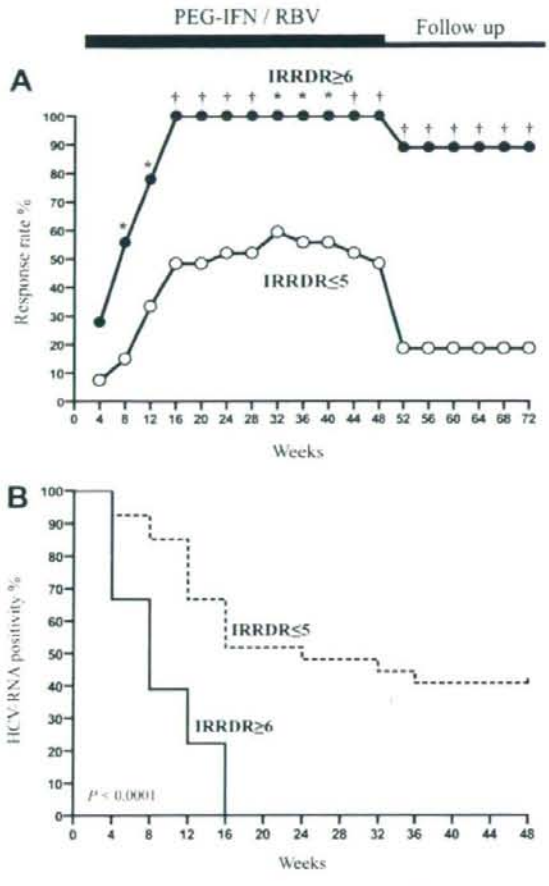

Fig. 3. Time course of HCV clearance during IFN/RBV treatment and follow-up period. (A) The viral clearance rates of patients infected with HCV isolates with six or more mutations in IRRDR (IRRDR ≥ 6) or five or fewer mutations (IRRDR ≤ 5) at 4-week intervals during the whole observation period. *$P < 0.01$; †, $P < 0.001$ (Fisher's exact probability test). (B) Kaplan-Meier HCV survival curve analysis based on serum HCV-RNA positivity during IFN/RBV treatment course (48 weeks) for HCV isolates with IRRDR of 6 or greater and IRRDR of 5 or fewer. $P < 0.0001$ (log-rank test).

after the initiation of treatment (Table 6). Most notably, all 18 patients infected with HCV isolates of IRRDR of 6 or greater achieved significant (≥1 log) reduction or disappearance of serum HCV core antigen titers 24 hours after the first dose of PEG-IFN/RBV.

Proposed Markers for Prediction of Various Virological Responses During PEG-IFN/RBV Combination Therapy. As described, IRRDR of 6 or greater and Ala^{2360} were statistically selected as independent SVR predictors. Therefore, we aimed to assess their predictability, in terms of positive and negative predictive values, for various virological responses to PEG-IFN/RBV combination therapy (Table 7). IRRDR greater than or equal to 6 could predict EVR(12w), ETR, and SVR with the positive predictive values of 78% ($P = 0.01$), 100% ($P = 0.000007$), and 89% ($P = 0.0007$), respectively. Moreover, the negative predictive value of IRRDR of 6 or greater for non-SVR was 81% ($P = 0.0008$). Thus, IRRDR of 6 or greater would be useful to predict not only SVR but also non-SVR. Similarly, Ala^{2360} could also predict ETR and SVR with positive predictive values of 92% ($P = 0.002$) and 77% ($P = 0.046$), respectively.

Discussion

A substantial proportion of HCV-1b–infected patients do not respond to IFN/RBV combination therapy. Given the significant side effects and high cost associated with this combination therapy, it would be of great utility if clinicians could predict, either before or during the treatment, which patients would, or would not, achieve SVR. Useful predictors of SVR must have a high positive predictive value; conversely, useful predictors of non-SVR must have high negative predictive value.[5] Most recent studies have focused on the possible correlation between the likelihood of achieving SVR and viral clearance kinetics during the first few months of the treatment.[25,26] Conversely, some studies dealt with the possible correlation between SVR and sequence variation within a part of NS5A, especially the V3 region.[12-20]

Table 6. Significant Correlation Between the Rapid Reduction of HCV Core Antigen Titers and IRRDR Sequence Variations

	No. of Patients With Significant Reduction of HCV Core Antigen Titers / No. of Total							
Criteria	24 Hours* (≥ 1 log)†	P Value‡	1 Week* (≥ 1 log)†	P Value‡	2 Weeks* (≥ 1.5 log)†	P Value‡	4 Weeks* (≥ 2 log)†	P Value‡
IRRDR ≥ 6	18/18	<0.0001	15/18	0.002	13/18	0.016	16/18	0.0007
IRRDR ≤ 5	10/27		9/27		9/27		10/27	

*Period after initiation of IFN/RBV therapy.

†Criteria of the significant reduction of HCV core antigen titers. Two (both at 24 hours and 1 week) and three patients (both at 2 and 4 weeks) who achieved disappearance of serum HCV core antigen were also considered to meet these criteria.

‡Fisher's exact test.

Abbreviations: IRRDR, interferon/ribavirin resistance-determining region; IFN/RBV, interferon/ribavirin.

Table 7. Positive Predictive Value, Negative Predictive Value, Sensitivity and Specificity of IRRDR ≥ 6 and Ala^{2360} on the Likelihood of Achieving Various Virological Responses

Virological Response	IRRDR ≥ 6				Ala^{2360}			
	PPV	NPV	Sensitivity	Specificity	PPV	NPV	Sensitivity	Specificity
EVR (12W)	78% (14/18)	67% (18/27)	61% (14/23)	82% (18/22)	69% (9/13)	56% (18/32)	39% (9/23)	82% (18/22)
ETR	100% (18/18)	56% (15/27)	58% (18/31)	100% (14/14)	92% (12/13)	41% (13/32)	39% (12/31)	93% (13/14)
SVR	89% (16/18)	81% (22/27)	76% (16/21)	92% (22/24)	77% (10/13)	66% (21/32)	48% (10/21)	88% (21/24)

Abbreviations: IRRDR, interferon/ribavirin resistance-determining region; Ala^{2360}, alanine at position 2360; EVR, early virological response; ETR, end-of-treatment response; SVR, sustained virological response; PPV, positive predictive value; NPV, negative predictive value.

We previously reported that a high degree of sequence variation (≥6 mutations) in IRRDR was significantly correlated with the EVR by week 16 in HCV-1b–infected patients treated with PEG-IFN/RBV combination therapy.[21] In the current follow-up study, we aimed to investigate whether the IRRDR sequence variation is correlated also with SVR. By using different statistical approaches, the results obtained clearly demonstrated that the high degree of sequence variation in IRRDR (IRRDR ≥6) significantly correlated with SVR, whereas the low degree of sequence variation in this region (IRRDR ≤5) correlated with non-SVR. Nearly two-thirds of patients with SVR had HCV of IRRDR of 6 or greater, whereas only 2 (8%) of 24 patients with non-SVR did ($P < 0.0001$) (Table 4). Notably, 16 of the 18 patients infected with HCV of IRRDR of 6 or greater achieved SVR. Accordingly, the positive predictive value and negative predictive value of IRRDR greater than or equal to 6 for SVR and non-SVR were 89% ($P = 0.0007$) and 81% ($P = 0.0008$), respectively (Table 7). Our current results thus strongly suggest that IRRDR greater than or equal to 6 would be a useful marker for prediction of SVR.

It was reported that the determination of HCV core antigen levels in the serum was an accurate and reliable alternative to monitor HCV RNA titers and that rapid reduction of HCV core antigen levels within a few weeks after the initiation of the therapy could predict treatment outcome in patients receiving PEG-IFN/RBV combination therapy.[27-29] Indeed, we found a strong association between the likelihood of achieving SVR and rapid reduction of HCV core antigen during the first 4 weeks of PEG-IFN/RBV combination therapy. More importantly, we found a significant correlation between the rapid reduction of HCV core antigen titers and the degree of sequence variation in IRRDR. Notably, all the patients infected with HCV of IRRDR greater than or equal to 6 showed a significant (≥1 log) reduction or disappearance of serum HCV core antigen titers 24 hours after the first dose of PEG-IFN/RBV (Table 6). This, in particular, suggests a possible influence of IRRDR of 6 or greater on HCV replication kinetics during IFN-based therapy because the direct effect of IFN begins a few hours after the first dose. Moreover, IRRDR greater than or equal to 6 was significantly associated with rapid clearance of serum HCV RNA as early as week 8 during PEG-IFN/RBV combination therapy (Fig. 3). These results collectively reinforce the possible correlation between the sequence variation in IRRDR and HCV clearance by the IFN-based therapy.

We also examined whether the criterion of IRRDR of 6 or greater was applicable to previously reported studies, for which information on both treatment outcome (responder versus nonresponder) and IRRDR sequences are available.[8,13] As shown in Table 8, the average numbers of amino acid variations from the same consensus sequence used in the current study were significantly larger for SVR than for non-SVR in a study with Japanese patients ($P = 0.003$)[8] and hovered at nearly a significant level in a study with European patients ($P = 0.06$).[13] More importantly, the criterion of IRRDR greater than or equal to 6 could significantly differentiate between responders and nonresponders in the Japanese study ($P = 0.003$) and also hovered at nearly a significant level in the European study ($P = 0.058$). It should be noted that, in the latter study, there were only three patients who had HCV with IRRDR of 6 or greater, all of whom became SVR. Taken together, these results suggest the useful application of IRRDR of 6 or greater as an SVR marker even in different geographical regions, although the prevalence of HCV with IRRDR of 6 or greater may vary with different regions of the world.

Although we observed significant correlation between the overall number of mutations in IRRDR and PEG-IFN/RBV responsiveness, we also found particular amino acid mutations, Ala^{2360} and Thr^{2378}, that were significantly associated with SVR (Table 4 and Fig. 2). In particular, Ala^{2360} was identified as an independent SVR marker. In this connection, it should be noted that four of five HCV isolates of IRRDR of 5 or less obtained from patients with SVR had either Ala^{2360} or Thr^{2378}. Furthermore, 20 (95%) of 21 HCV isolates obtained from pa-

Table 8. Comparative Analysis of the Mean Numbers of aa Mutations in IRRDR in Previously Reported Japanese and European Studies

Study	Factor	SVR	Non-SVR	P Value
Enomoto et al.[8]	No. of IRRDR mutations	7.6 ± 2.6*	3.7 ± 2.0	0.003†
	No. of patients with IRRDR ≥ 6	8	1	0.003‡
	IRRDR ≤ 5	1	8	
Duverlie et al.[13]	No. of IRRDR mutations	5.6 ± 2.3	4.2 ± 0.8	0.06†
	No. of patients with IRRDR ≥ 6	3	0	0.056‡
	IRRDR ≤ 5	5	11	
This study	No. of IRRDR mutations	6.1 ± 2.1	3.9 ± 1.4	0.0006†
	No. of patients with IRRDR ≥ 6	16	2	< 0.0001‡
	IRRDR ≤ 5	5	22	

NOTE. Same consensus sequence was used in this comparative analysis.
*Mean ± SD.
†Student *t* test.
‡Fisher's exact test.
Abbreviations: aa, amino acid; IRRDR, interferon/ribavirin resistance-determining region; SVR, sustained virological response.

tients with SVR had either one of the three factors (IRRDR ≥6, Ala^{2360}, or Thr^{2378}). To our knowledge, there is no known CD4 or CD8 epitope(s) in IRRDR so far reported. Interestingly, however, Neumann-Haefelin et al.[30] recently identified an HLA-A26 $CD8^+$ T-cell epitope located at position 2416, 37 aa distant from IRRDR. This epitope was shown to be targeted in all patients with acute resolving HCV infection examined. Further studies are needed to elucidate the role(s) for the distal carboxy terminal region of NS5A, including IRRDR, in both IFN/RBV responsiveness and T cell–mediated virus clearance.

In conclusion, our results suggest that a high degree of sequence variation in IRRDR (IRRDR ≥6), and a particular aa mutation (Ala^{2360}) to a lesser extent, would be a useful marker to predict SVR.

References

1. Hoofnagle JH, Seeff LB. Peginterferon and ribavirin for chronic hepatitis C. N Engl J Med 2006;355:2444-2451.
2. Pawlotsky JM. Therapy of hepatitis C: from empiricism to eradication. HEPATOLOGY 2006;43:S207-S220.
3. Manns MP, McHutchison JG, Gordon SC, Rustgi VK, Shiffman M, Reindollar R, et al. Peginterferon alfa-2b plus ribavirin compared with interferon alfa-2b plus ribavirin for initial treatment of chronic hepatitis C: a randomised trial. Lancet 2001;358:958-965.
4. Fried MW, Shiffman ML, Reddy KR, Smith C, Marinos G, Goncales FL Jr, et al. Peginterferon alfa-2a plus ribavirin for chronic hepatitis C virus infection. N Engl J Med 2002;347:975-982.
5. Ferenci P, Fried MW, Shiffman ML, Smith CI, Marinos G, Goncales FL Jr, et al. Predicting sustained virological responses in chronic hepatitis C patients treated with peginterferon alfa-2a (40 KD)/ribavirin. J Hepatol 2005;43:425-433.
6. Ferenci P. Predictors of response to therapy for chronic hepatitis C. Semin Liver Dis 2004;24(Suppl 2):25-31.
7. Welker MW, Hofmann WP, Welsch C, von Wagner M, Herrmann E, Lengauer T, et al. Correlation of amino acid variations within nonstructural 4B protein with initial viral kinetics during interferon-alpha-based therapy in HCV-1b-infected patients. J Viral Hepatol 2007;14:338-349.
8. Enomoto N, Sakuma I, Asahina Y, Kurosaki M, Murakami T, Yamamoto C, et al. Comparison of full-length sequences of interferon-sensitive and resistant hepatitis C virus 1b: sensitivity to interferon is conferred by amino acid substitutions in the NS5A region. J Clin Invest 1995;96:224-230.
9. Enomoto N, Sakuma I, Asahina Y, Kurosaki M, Murakami T, Yamamoto C, et al. Mutations in the nonstructural protein 5A gene and response to interferon in patients with chronic hepatitis C virus 1b infection. N Engl J Med 1996;334:77-81.
10. Gale MJ Jr, Korth MJ, Tang NM, Tan SL, Hopkins DA, Dever TE, et al. Evidence that hepatitis C virus resistance to interferon is mediated through repression of the PKR protein kinase by the nonstructural 5A protein. Virology 1997;230:217-227.
11. Gale MJ Jr, Korth MJ, Katze MG. Repression of the PKR protein kinase by the hepatitis C virus NS5A protein: a potential mechanism of interferon resistance. Clin Diagn Virol 1998;10:157-162.
12. Nousbaum J, Polyak SJ, Ray SC, Sullivan DG, Larson AM, Carithers RL, Jr, Gretch DR. Prospective characterization of full-length hepatitis C virus NS5A quasispecies during induction and combination antiviral therapy. J Virol 2000;74:9028-9038.
13. Duverlie G, Khorsi H, Castelain S, Jaillon O, Izopet J, Lunel F, et al. Sequence analysis of the NS5A protein of European hepatitis C virus 1b isolates and relation to interferon sensitivity. J Gen Virol 1998;79 (Pt 6):1373-1381.
14. Layden-Almer JE, Kuiken C, Ribeiro RM, Kunstman KJ, Perelson AS, Layden TJ, Wolinsky SM. Hepatitis C virus genotype 1a NS5A pretreatment sequence variation and viral kinetics in African American and white patients. J Infect Dis 2005;192:1078-1087.
15. Vuillermoz I, Khattab E, Sablon E, Ottevaere I, Durantel D, Vieux C, et al. Genetic variability of hepatitis C virus in chronically infected patients with viral breakthrough during interferon-ribavirin therapy. J Med Virol 2004; 74:41-53.
16. Puig-Basagoiti F, Forns X, Furcic I, Ampurdanes S, Gimenez-Barcons M, Franco S, et al. Dynamics of hepatitis C virus NS5A quasispecies during interferon and ribavirin therapy in responder and non-responder patients with genotype 1b chronic hepatitis C. J Gen Virol 2005;86:1067-1075.
17. Sarrazin C, Herrmann E, Bruch K, Zeuzem S. Hepatitis C virus nonstructural 5A protein and interferon resistance: a new model for testing the reliability of mutational analyses. J Virol 2002;76:11079-11090.
18. Murphy MD, Rosen HR, Marousek GI, Chou S. Analysis of sequence configurations of the ISDR, PKR-binding domain, and V3 region as predictors of response to induction interferon-alpha and ribavirin therapy in chronic hepatitis C infection. Dig Dis Sci 2002;47:1195-1205.
19. Veillon P, Payan C, Le Guillou-Guillemette H, Gaudy C, Lunel F. Quasispecies evolution in NS5A region of hepatitis C virus genotype 1b during interferon or combined interferon-ribavirin therapy. World J Gastroenterol 2007;13:1195-1203.

20. Wohnsland A, Hofmann WP, Sarrazin C. Viral determinants of resistance to treatment in patients with hepatitis C. Clin Microbiol Rev 2007;20:23-38.
21. El-Shamy A, Sasayama M, Nagano-Fujii M, Sasase N, Imoto S, Kim SR, et al. Prediction of efficient virological response to pegylated interferon/ribavirin combination therapy by NS5A sequences of hepatitis c virus and anti-NS5A antibodies in pre-treatment sera. Microbiol Immunol 2007;51:471-482.
22. Okamoto H, Sugiyama Y, Okada S, Kurai K, Akahane Y, Sugai Y, et al. Typing hepatitis C virus by polymerase chain reaction with type-specific primers: application to clinical surveys and tracing infectious sources. J Gen Virol 1992;73(Pt 3):673-679.
23. Lusida MI, Nagano-Fujii M, Nidom CA, Soetjipto, Handajani R, Fujita T, et al. Correlation between mutations in the interferon sensitivity-determining region of NS5A protein and viral load of hepatitis C virus subtypes 1b, 1c, and 2a. J Clin Microbiol 2001;39:3858-3864.
24. Kato N, Hijikata M, Ootsuyama Y, Nakagawa M, Ohkoshi S, Sugimura T, et al. Molecular cloning of the human hepatitis C virus genome from Japanese patients with non-A, non-B hepatitis. Proc Natl Acad Sci U S A 1990;87:9524-9528.
25. Lukasiewicz E, Hellstrand K, Westin J, Ferrari C, Neumann AU, Pawlotsky JM, et al. Predicting treatment outcome following 24 weeks peginterferon alpha-2a/ribavirin therapy in patients infected with HCV genotype 1: utility of HCV-RNA at day 0, day 22, day 29, and week 6. HEPATOLOGY 2007;45:258-259.
26. Jensen DM, Morgan TR, Marcellin P, Pockros PJ, Reddy KR, Hadziyannis SJ, et al. Early identification of HCV genotype 1 patients responding to 24 weeks peginterferon alpha-2a (40 kd)/ribavirin therapy. HEPATOLOGY 2006;43:954-960.
27. Maynard M, Pradat P, Berthillon P, Picchio G, Voirin N, Martinot M, et al. Clinical relevance of total HCV core antigen testing for hepatitis C monitoring and for predicting patients' response to therapy. J Viral Hepat 2003;10:318-323.
28. Bouvier-Alias M, Patel K, Dahari H, Beaucourt S, Larderie P, Blatt L, et al. Clinical utility of total HCV core antigen quantification: a new indirect marker of HCV replication. HEPATOLOGY 2002;36:211-218.
29. Veillon P, Payan C, Picchio G, Maniez-Montreuil M, Guntz P, Lunel F. Comparative evaluation of the total hepatitis C virus core antigen, branched-DNA, and amplicor monitor assays in determining viremia for patients with chronic hepatitis C during interferon plus ribavirin combination therapy. J Clin Microbiol 2003;41:3212-3220.
30. Neumann-Haefelin C, Killinger T, Timm J, Southwood S, McKinney D, Blum HE, et al. Absence of viral escape within a frequently recognized HLA-A26-restricted CD8+ T-cell epitope targeting the functionally constrained hepatitis C virus NS5A/5B cleavage site. J Gen Virol 2007;88:1986-1991.

JOURNAL OF VIROLOGY, Nov. 2008, p. 10375–10385 Vol. 82, No. 21
0022-538X/08/$08.00+0 doi:10.1128/JVI.00395-08

Hepatitis C Virus Infection Induces Apoptosis through a Bax-Triggered, Mitochondrion-Mediated, Caspase 3-Dependent Pathway▽

Lin Deng,[1] Tetsuya Adachi,[1] Kikumi Kitayama,[1] Yasuaki Bungyoku,[1] Sohei Kitazawa,[2] Satoshi Ishido,[3] Ikuo Shoji,[1] and Hak Hotta[1]*

Divisions of Microbiology[1] and Molecular Pathology,[2] Kobe University Graduate School of Medicine, 7-5-1 Kusunoki-cho, Chuo-ku, Kobe 650-0017, and Laboratory for Infectious Immunity, Riken Research Center for Allergy and Immunology, 1-7-22 Suehiro-cho, Tsurumi-ku, Yokohama, Kanagawa 230-0045,[3] Japan

Received 23 February 2008/Accepted 20 August 2008

We previously reported that cells harboring the hepatitis C virus (HCV) RNA replicon as well as those expressing HCV NS3/4A exhibited increased sensitivity to suboptimal doses of apoptotic stimuli to undergo mitochondrion-mediated apoptosis (Y. Nomura-Takigawa, et al., J. Gen. Virol. 87:1935–1945, 2006). Little is known, however, about whether or not HCV infection induces apoptosis of the virus-infected cells. In this study, by using the chimeric J6/JFH1 strain of HCV genotype 2a, we demonstrated that HCV infection induced cell death in Huh7.5 cells. The cell death was associated with activation of caspase 3, nuclear translocation of activated caspase 3, and cleavage of DNA repair enzyme poly(ADP-ribose) polymerase, which is known to be an important substrate for activated caspase 3. These results suggest that HCV-induced cell death is, in fact, apoptosis. Moreover, HCV infection activated Bax, a proapoptotic member of the Bcl-2 family, as revealed by its conformational change and its increased accumulation on mitochondrial membranes. Concomitantly, HCV infection induced disruption of mitochondrial transmembrane potential, followed by mitochondrial swelling and release of cytochrome *c* from mitochondria. HCV infection also caused oxidative stress via increased production of mitochondrial superoxide. On the other hand, HCV infection did not mediate increased expression of glucose-regulated protein 78 (GRP78) or GRP94, which are known as endoplasmic reticulum (ER) stress-induced proteins; this result suggests that ER stress is not primarily involved in HCV-induced apoptosis in our experimental system. Taken together, our present results suggest that HCV infection induces apoptosis of the host cell through a Bax-triggered, mitochondrion-mediated, caspase 3-dependent pathway(s).

Hepatitis C virus (HCV) often establishes persistent infection to cause chronic hepatitis, liver cirrhosis, and hepatocellular carcinoma, which is a significant health problem around the world (56). Although the exact mechanisms of HCV pathogenesis, such as viral persistence, liver cell injury, and carcinogenesis, are not fully understood yet, an accumulating body of evidence suggests that apoptosis of hepatocytes is significantly involved in the pathogenesis of HCV (1, 2, 9). It is widely accepted that apoptosis of virus-infected cells is an important strategy of the host to protect itself against viral infections. Apoptotic cell death can be mediated either by the host immune responses through the function of virus-specific cytotoxic T lymphocytes and/or by viral proteins themselves that trigger an apoptotic pathway(s) of the host cell.

Apoptotic pathways can be classified into two groups: the mitochondrial death (intrinsic) pathway and the extrinsic cell death pathway initiated by the tumor necrosis factor (TNF) family members (31, 63). Mitochondrion-mediated apoptosis is initiated by a variety of apoptosis-inducing signals that cause the imbalance of the major apoptosis regulator, the proteins of the Bcl-2 family, such as Bcl-2, Bax, and Bid. For example, the proapoptotic protein Bax accumulates on mitochondria after being activated and triggers an increase in the permeability of the outer mitochondrial membrane. Consequently, the mitochondria release cytochrome *c* and other key molecules that facilitate apoptosome formation to activate caspase 9. This, in turn, activates downstream death programs, such as caspase 3 and poly(ADP-ribose) polymerase (PARP). The mitochondria also release apoptosis-inducing factor and endonuclease G to facilitate caspase-independent apoptosis. On the other hand, the extrinsic cell death pathway involves the activation of caspase 8 through binding to the adaptor protein Fas-associated protein with death domain (FADD), which in turn activates caspase 3 to facilitate cell death.

There have been many studies regarding the HCV protein(s) that is directly involved in apoptosis, identifying the protein as either proapoptotic or antiapoptotic, and some data are inconsistent. For example, core (5, 13, 36, 73), E1 (15, 16), E2 (12), NS3 (48), NS4A (43), and NS5A and NS5B (57) have been reported to induce apoptosis. On the other hand, there are reports showing that core (40, 49, 51), E2 (35), NS2 (21), NS3 (58), and NS5A (33, 67) function as antiapoptotic proteins. However, whether the virus as a whole is proapoptotic or antiapoptotic needs to be studied in the context of virus replication, which is believed to be much more dynamic than mere expression of a viral protein(s).

We previously reported that replication of an HCV RNA replicon rendered the host cell prone to undergoing mitochondrion-mediated apoptosis upon suboptimal doses of apoptosis-inducing stimuli (43). Recently, an efficient virus infection system using a particular clone of HCV genotype 2a and a highly permissive human hepatocellular carcinoma-derived cell line

* Corresponding author. Mailing address: Division of Microbiology, Kobe University Graduate School of Medicine, 7-5-1 Kusunoki-cho, Chuo-ku, Kobe 650-0017, Japan. Phone: 81-78-382-5500. Fax: 81-78-382-5519. E-mail: hotta@kobe-u.ac.jp.

▽ Published ahead of print on 3 September 2008.

has been developed (37, 38, 66, 71). In this study, by using the virus infection system, we examined the possible effect of HCV infection on the fate of the host cell. We report here that HCV infection induces apoptosis via the mitochondrion-mediated pathway, as demonstrated by the increased accumulation of the proapoptotic protein Bax on the mitochondria, decreased mitochondrial transmembrane potential, and mitochondrial swelling, which result in the release of cytochrome *c* from the mitochondria and the activation of caspase 3.

MATERIALS AND METHODS

Cells. The Huh7.5 cell line (6), a highly HCV-susceptible subclone of Huh7 cells, was a kind gift from C. M. Rice, Center for the Study of Hepatitis C, The Rockefeller University. The cells were propagated in Dulbecco's modified Eagle medium supplemented with 10% heat-inactivated fetal bovine serum and 0.1 mM nonessential amino acids.

Virus. The virus stock used in this study was prepared as described below. The pFL-J6/JFH1 plasmid, encoding the entire viral genome of a chimeric strain of HCV genotype 2a, J6/JFH1 (37), was kindly provided by C. M. Rice. The plasmid was linearized by XbaI digestion and in vitro transcribed by using T7 RiboMAX (Promega, Madison, WI) to generate the full-length viral genomic RNA. The in vitro-transcribed RNA (10 μg) was transfected into Huh7.5 cells by means of electroporation (975 μF, 270 V) using Gene Pulser (Bio-Rad, Hercules, CA). The cells were then cultured in complete medium, and the supernatant was propagated as an original virus (J6/JFH1-passage 1 [J6/JFH1-P1]). Since the infectious titer of the original virus was not high enough for infection of all the cells in the culture at once, an adapted strain of the virus was obtained by passaging the virus-infected cells 47 times. The adapted virus (J6/JFH1-P47), which is a pool of adapted mutants, possesses 10 amino acid mutations (K78E, T396A, T416A, N534H, A712V, Y852H, W879R, F2281L, M2876L, and T2925A) and a single nucleotide mutation in the 5′-untranslated region (U146A) and produces a much higher titer of infectivity in Huh7.5 cell cultures than the original J6/JFH1-P1 (our unpublished data). Virus infection was performed at a multiplicity of infection of 2.0. Culture supernatants of uninfected cells served as a control (mock preparation).

Virus infectivity was measured by indirect immunofluorescence analysis, as described below, and expressed as cell-infecting units/ml.

Cell viability/proliferation assay. Huh7.5 cells were seeded in 96-well plates at a density of 1.0×10^4 cells/well and cultured overnight. The cells were then infected with the virus or the mock preparation, and, at different time points, cell viability/proliferation was determined by the WST-1 assay (Roche, Mannheim, Germany), as described previously (43).

Detection of apoptosis. The degree of apoptosis was measured by using a Cell Death Detection ELISA^{Plus} kit (Roche), which is based on the determination of cytoplasmic histone-associated DNA fragments, according to the manufacturer's protocol. In brief, cells cultured in a 96-well plate were centrifuged at $200 \times g$ for 10 min at 4°C to remove the supernatant. After the cells were lysed with lysis buffer, the plate was centrifuged at $200 \times g$ for 10 min to separate the cytoplasmic and nuclear fractions. Twenty microliters of supernatant was placed in each well of a streptavidin-coated 96-well plate. Subsequently, a mixture of biotin-labeled anti-histone antibody and peroxidase-labeled anti-DNA antibody was added and wells were incubated for 2 h at room temperature. After wells were washed three times to remove the unbound components, peroxidase activities were determined photometrically with 2,2′-azino-diethyl-benzthiazolin sulfonate as a substrate and measured by using a microplate reader (Bio-Rad).

Caspase enzymatic activities. Activities of caspase 3, 8, and 9 were measured by using Caspase-Glo 3/7, 8, and 9 assays (Promega), respectively, according to the manufacturer's instructions. In brief, a proluminescence caspase 3/7, 8, or 9 substrate, which consists of aminoluciferin (substrate for luciferase) and the tetrapeptide sequence DEVD, LETD, or LEHD (cleavage site for caspase 3/7, 8, or 9, respectively), was added to cultured cells in each well of a 96-well plate, and the plate was incubated for 30 min at room temperature. In the presence of caspase 3/7, 8, or 9, aminoluciferin was liberated from the proluminescence substance and utilized as a substrate for the luciferase reaction. The resultant luminescence in relative light units was measured by using a Luminescencer-JNR AB-2100 (Atto, Tokyo, Japan).

Cell fractionation. Cells were fractionated by using a mitochondrial isolation kit (Pierce, Rockford, IL), according to the manufacturer's instructions. Briefly, 2×10^7 cells were harvested and suspended in reagent A containing a protease inhibitor cocktail (Roche). The cell suspension was mixed with buffer B, vortexed for 5 min, and then mixed with reagent C. The nuclei and unbroken cells were removed by centrifugation at $700 \times g$ for 10 min at 4°C, and the supernatant was used as cell lysate. The cell lysate was further centrifuged at $3,000 \times g$ for 15 min at 4°C. The pellet obtained, which was considered the mitochondrial fraction, was washed once with reagent C and dissolved in a lysis buffer containing 10 mM Tris-HCl (pH 7.5), 150 mM NaCl, 1 mM EDTA, 1% NP-40, and a protease inhibitor cocktail. The remaining supernatant was further centrifuged at $100,000 \times g$ for 30 min at 4°C, and the resultant supernatant was collected as a cytosolic fraction.

To verify successful mitochondrial fractionation, the cytosolic and mitochondrial fractions were analyzed by immunoblotting, as described below, using antibody against Tim23, a mitochondrion-specific protein.

Analysis of the mitochondrial transmembrane potential. The mitochondrial transmembrane potential was measured by flow cytometry using the cationic lipophilic green fluorochrome rhodamine 123 (Rho123; Sigma, St. Louis, MO), as described previously (43). Briefly, cells (7×10^5) were harvested, washed twice with phosphate-buffered saline (PBS), and incubated with Rho123 (0.5 μg/ml) at 37°C for 25 min. The cells were then washed twice with PBS, and Rho123 intensity was analyzed by a flow cytometer (Becton Dickinson, San Jose, CA). A total of 10,000 events were collected per sample. Mean fluorescence intensities were measured by calculating the geometric mean for each histogram peak.

Detection of morphological changes of the mitochondria. Mitochondrial morphology was analyzed by two different methods. (i) For fluorescence microscopy, Huh7.5 cells seeded on glass coverslips in a 24-well plate were incubated for 30 min at 37°C with 100 nM MitoTracker (Molecular Probes, Eugene, OR). After being washed twice with PBS, the cells were fixed with 3.7% paraformaldehyde and observed under a confocal laser scanning microscope (Carl Zeiss, Oberkochen, Germany). When needed, the fixed cells were subjected to indirect immunofluorescence to confirm HCV infection, as described below. (ii) Electron microscopy was performed as described previously (23, 43). In brief, cells were fixed with 4% paraformaldehyde and 0.2% glutaraldehyde for 30 min at room temperature. After being washed with PBS, the cells were collected, dehydrated in a series of 70%, 80%, and 90% ethanol, embedded in LR White resin (London Resin, Berkshire, United Kingdom), and kept at −20°C for 2 days to facilitate resin polymerization. After ultrathin sectioning, samples were etched in 3% H_2O_2 for 5 min at room temperature and washed with PBS. Sections were stained with uranyl acetate and lead citrate and observed under a transmission electron microscope (JEM 1299EX; JOEL, Tokyo, Japan).

Detection of mitochondrial superoxide. Cells seeded on glass coverslips in a 24-well plate were incubated with 5 μM MitoSOX Red (Molecular Probes) at 37°C for 10 min. After being washed with warm Hanks' balanced salt solution with calcium and magnesium (Invitrogen, Carlsbad, CA), the cells were fixed with 3.7% paraformaldehyde and observed under a confocal laser scanning microscope (Carl Zeiss). When needed, the fixed cells were subjected to indirect immunofluorescence to confirm HCV infection, as described below.

Indirect immunofluorescence. Cells seeded on glass coverslips in a 24-well plate at a density of 6×10^4 cells/well were infected with HCV or left uninfected. At different time points after virus infection, the cells were fixed with 3.7% paraformaldehyde in PBS for 15 min at room temperature and permeabilized in 0.1% Triton X-100 in PBS for 15 min at room temperature. After being washed with PBS twice, cells were consecutively stained with primary and secondary antibodies. Primary antibodies used were anti-active caspase 3 rabbit polyclonal antibody (Promega) and an HCV-infected patient's serum. Secondary antibodies used were Cy3-conjugated donkey anti-rabbit immunoglobulin G (IgG; Chemicon, Temecula, CA), Alexa Fluor 594-conjugated goat anti-human IgG (Molecular Probes), and fluorescein isothiocyanate (FITC)-conjugated goat anti-human IgG (MBL, Nagoya, Japan). The cells were washed with PBS, counterstained with Hoechst 33342 solution (Molecular Probes) at room temperature for 10 min, mounted on glass slides, and observed under a confocal laser scanning microscope (Carl Zeiss). The specificity of this immunostaining was confirmed by using mouse monoclonal antibody against HCV core protein (C7-50; Abcam, Tokyo, Japan).

To analyze the possible localization of the activated Bax on mitochondrial membranes, cells were incubated with MitoTracker and subjected to immunofluorescence analysis using rabbit polyclonal antibody against activated Bax (NT antibody; Upstate, Lake Placid, NY). This antibody is directed toward N-terminal residues 1 to 21 of Bax in an N-terminal conformation-dependent manner and specifically recognizes the active form of Bax, in which this segment is exposed in response to apoptotic stimuli (64).

Immunoblotting. Cells were lysed in a buffer containing 10 mM Tris-HCl (pH 7.5), 150 mM NaCl, 1 mM EDTA, 1% NP-40, and a protease inhibitor cocktail (Roche). After two freeze-thaw cycles, cell debris was removed by

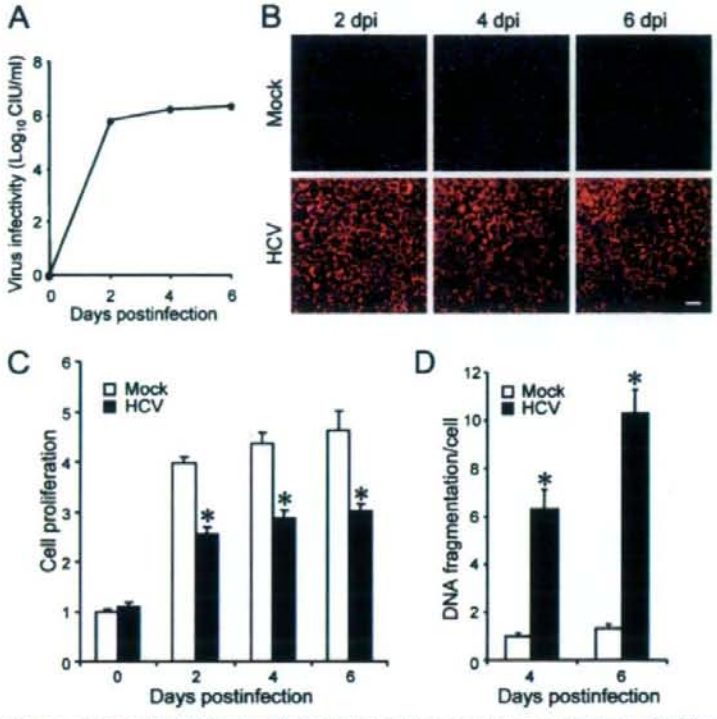

FIG. 1. HCV infection induces apoptosis in Huh7.5 cells. (A) Virus infectivity in the culture supernatants of HCV-infected cells. (B) Detection of HCV antigens in the cells. Huh7.5 cells mock inoculated or inoculated with HCV were subjected to indirect immunofluorescence analysis to detect HCV antigens (red staining) using an HCV-infected patient's serum and Alexa Fluor 594-conjugated goat anti-human IgG at 2, 4, and 6 days postinfection (dpi). Nuclei were counterstained with Hoechst 33342 (blue staining). Scale bar, 50 μm. (C) Cell viability/proliferation was measured for HCV-infected cultures and the mock-inoculated controls. Proliferation of the control cells at day 0 postinfection was arbitrarily expressed as 1.0. Data represent means ± standard deviations (SD) of three independent experiments. *, $P < 0.01$, compared with the control. (D) DNA fragmentation was measured as an index of apoptotic cell death for HCV-infected cultures and the mock-inoculated controls. DNA fragmentation of the control cells at 4 days postinfection was arbitrarily expressed as 1.0. Data represent means ± SD of three independent experiments. *, $P < 0.01$, compared with the control.

centrifugation. Protein quantification was carried out using a bicinchoninic acid protein assay kit (Pierce). Equal amounts of soluble proteins (4 to 20 μg) were subjected to sodium dodecyl sulfate-polyacrylamide gel electrophoresis and transferred onto a polyvinylidene diffluoride membrane (Millipore, Bedford, MA), which was then incubated with the respective primary antibody. The primary antibodies used were mouse monoclonal antibodies against cytochrome *c* (A-8; Santa Cruz Biotechnology, Santa Cruz, CA), HCV NS3 (Chemicon), Tim23, Bax and Bcl-2 (BD Biosciences Pharmingen, San Diego, CA); rabbit polyclonal antibodies against Bak (Upstate), caspase 3, and PARP (Cell Signaling Technology, Danvers, MA); and goat polyclonal antibodies against glucose-regulated protein 78 (GRP78) and GRP94 (Santa Cruz Biotechnology). Horseradish peroxidase-conjugated goat anti-mouse IgG (MBL), goat anti-rabbit IgG (Bio-Rad), and donkey anti-goat IgG (Santa Cruz Biotechnology) were used as secondary antibodies. In some experiments, a commercial kit that facilitates the antigen-antibody reaction (Can Get Signal; Toyobo, Osaka, Japan) was used to obtain stronger signals. The respective protein bands were visualized by means of an enhanced chemiluminescence (GE Healthcare, Buckinghamshire, United Kingdom), and the intensity of each band was quantified by using NIH Image J. Protein loading was normalized by probing with goat antibody against actin (Santa Cruz Biotechnology) as a primary antibody.

Statistical analysis. The two-tailed Student *t* test was applied to evaluate the statistical significance of differences measured from the data sets. A *P* value of <0.05 was considered statistically significant.

RESULTS

HCV infection induces caspase 3-dependent apoptosis in Huh7.5 cells. We first examined virus growth in Huh7.5 cells. HCV grew efficiently in the culture, and virus titers in the supernatant reached a plateau level at 2 days postinfection (Fig. 1A). Immunofluorescence analysis revealed that >95% of the cells were infected with HCV on the same day (Fig. 1B). To examine the possible impact of HCV infection on the cells, we measured the cell viability/proliferation at 0, 2, 4, and 6 days postinfection. As shown in Fig. 1C, the proliferation of HCV-infected cells was significantly slower than that of the mock-infected control. Similar results were obtained when the parental Huh7 cells were used for HCV infection (data not shown). The observed delay in cell proliferation was associated with an increase in cell death, seen as cell rounding and floating in the culture (data not shown) and in cellular DNA fragmentation (Fig. 1D). As DNA fragmentation is a hallmark of apoptosis, our data suggest that HCV infection induces apoptosis in Huh7.5 cells.

The J6/JFH1-P47 strain of HCV used in this study possesses adaptive mutations compared to the original strain (J6/JFH1-P1). Therefore, we compared the impacts of the two strains on cell viability/proliferation and DNA fragmentation. While both strains caused inhibition of cell proliferation and an increase in DNA fragmentation, J6/JFH1-P47 appeared to exert a stronger cytopathic effect than J6/JFH-P1 (data not shown).

To further verify that HCV infection induces apoptotic cell death, we analyzed caspase 3 activities in HCV-infected Huh7.5 cells and the mock-infected control. As shown in Fig. 2A, caspase 3 activities in HCV-infected cells increased to levels that were 2.2, 6.0, and 12 times higher than that in the control cells at 2, 4, and 6 days postinfection, respectively. We also examined HCV-induced caspase 3 activation by immunoblot analysis. Activation of caspase 3 requires proteolytic processing of its inactive proenzyme into the active 17-kDa and 12-kDa subunit proteins. The anti-caspase 3 antibody used in this analysis recognizes 35-kDa procaspase 3 and the 17-kDa subunit protein. At 6 days postinfection, activated caspase 3 was detected in HCV-infected cells but not in the mock-infected control (Fig. 2B, second row from the top). Analysis of the death substrate PARP, which is a key substrate for active caspase 3 (61), also demonstrated that the uncleaved PARP (116 kDa) was proteolytically cleaved to generate the 89-kDa fragment in HCV-infected cells but not in the mock-infected control (Fig. 2B, third row). Cleavage of PARP facilitates cellular disassembly and serves as a marker of cells undergoing apoptosis (44).

In order to further confirm these observations, indirect immunofluorescence staining was performed by using an anti-active caspase 3 antibody that specifically recognizes the newly exposed C terminus of the 17-kDa fragment of caspase 3 but not the inactive precursor form. As shown in Fig. 2C, the activated form of caspase 3 was clearly observed in HCV-infected cells but not in the mock-infected control at 6 days postinfection. The activation of caspase 3 was observed also at 4 days postinfection (data not shown). We found that caspase 3 activation was detectable in 12% and 21% of HCV antigen-positive cells at 4 and 6 days postinfection, respectively, whereas it was detectable only minimally in mock-infected cells at the same time points (Fig. 2D). These results strongly suggest that HCV-induced cell death is caused by caspase 3-dependent apoptosis. We also observed nuclear translocation of active caspase 3 in HCV-infected cells (Fig. 2E). This result is consistent with previous reports (28, 70) that activated caspase 3 is located not only in the cytoplasm but also in the nuclei of apoptotic cells. Concomitantly, nuclear condensation and shrinkage were clearly observed in the caspase 3-activated cells. As the activation and nuclear translocation of caspase 3 occur before the appearance of the nuclear change, not all caspase 3-activated cells exhibited the typical nuclear changes. Taken together, these results indicate that HCV-induced apoptosis is associated with activation and nuclear translocation of caspase 3.

HCV infection induces the activation of the proapoptotic protein Bax. The proteins of the Bcl-2 family are known to directly regulate mitochondrial membrane permeability and induction of apoptosis (63). Therefore, we examined the expression levels of proapoptotic proteins, such as Bax and Bak, and antiapoptotic protein Bcl-2 in HCV-infected Huh7.5 cells and the mock-infected control. The result showed that expression levels of Bak or Bcl-2 did not differ significantly between HCV-infected cells and the control. Interestingly, however, Bax accumulated on the mitochondria in HCV-infected cells to a larger extent than in the mock-infected control (Fig. 3A), with the average amount of mitochondrion-associated Bax in HCV-infected cells being 2.7 times larger than that in the control cells at 6 days postinfection (Fig. 3B).

In response to apoptotic stimuli, Bax undergoes a conformational change to expose its N and C termini, which facilitates translocation of the protein to the mitochondrial outer membrane (32). Thus, the conformational change of Bax represents a key step for its activation and subsequent apoptosis. We therefore investigated the possible conformational change of Bax in HCV-infected cells by using a conformation-specific NT antibody that specifically recognizes the Bax protein with an exposed N terminus. As shown in Fig. 3C, Bax staining with the conformation-specific NT antibody was readily detectable in HCV-infected cells at 6 days postinfection whereas there was no detectable staining with the same antibody in the mock-infected control. Moreover, the activated Bax was shown to be colocalized with MitoTracker, a marker for mitochondria, in HCV-infected cells. The conformational change of Bax was observed in 10% and 15% of HCV-infected cells at 4 and 6 days postinfection, respectively (Fig. 3D). This result was consistent with what was observed for caspase 3 activation in HCV-infected cells (Fig. 2D). Taken together, these results suggest that HCV infection triggers conformational change and mitochondrial accumulation of Bax, which lead to the activation of the mitochondrial apoptotic pathway.

HCV infection induces the disruption of the mitochondrial transmembrane potential, release of cytochrome *c* from mitochondria, and activation of caspase 9. The accumulation of Bax on the mitochondria is known to decrease the mitochondrial transmembrane potential and increase its permeability, which result in the release of cytochrome *c* and other key molecules from the mitochondria to the cytoplasm to activate caspase 9. Therefore, we examined the possible effect of HCV infection on mitochondrial transmembrane potential in Huh7.5 cells. Disruption of the mitochondrial transmembrane potential was indicated by decreased Rho123 retention and, hence, decreased fluorescence. As shown in Fig. 4, HCV-infected cells showed ~50% and ~70% reductions in Rho123 fluorescence intensity compared with the mock-infected control at 4 and 6 days postinfection, respectively.

Recent studies have indicated that loss of mitochondrial membrane potential leads to mitochondrial swelling, which is often associated with cell injury (27, 50). Also, we and other investigators have reported that HCV NS4A (43), core (53), and p7 (22) target mitochondria. We therefore analyzed the effect of HCV infection on mitochondrial morphology. Confocal fluorescence microscopic analysis using MitoTracker revealed that mitochondria began to undergo morphological changes at 4 days postinfection and that approximately 40% of HCV-infected cells exhibited mitochondrial swelling and/or aggregation compared with the mock-infected control at 6 days postinfection (Fig. 5A and B). It should also be noted that mitochondrial swelling and/or aggregation was seen in a region different from the "membranous web," where the HCV replication complexes accumulate to show stronger expression of

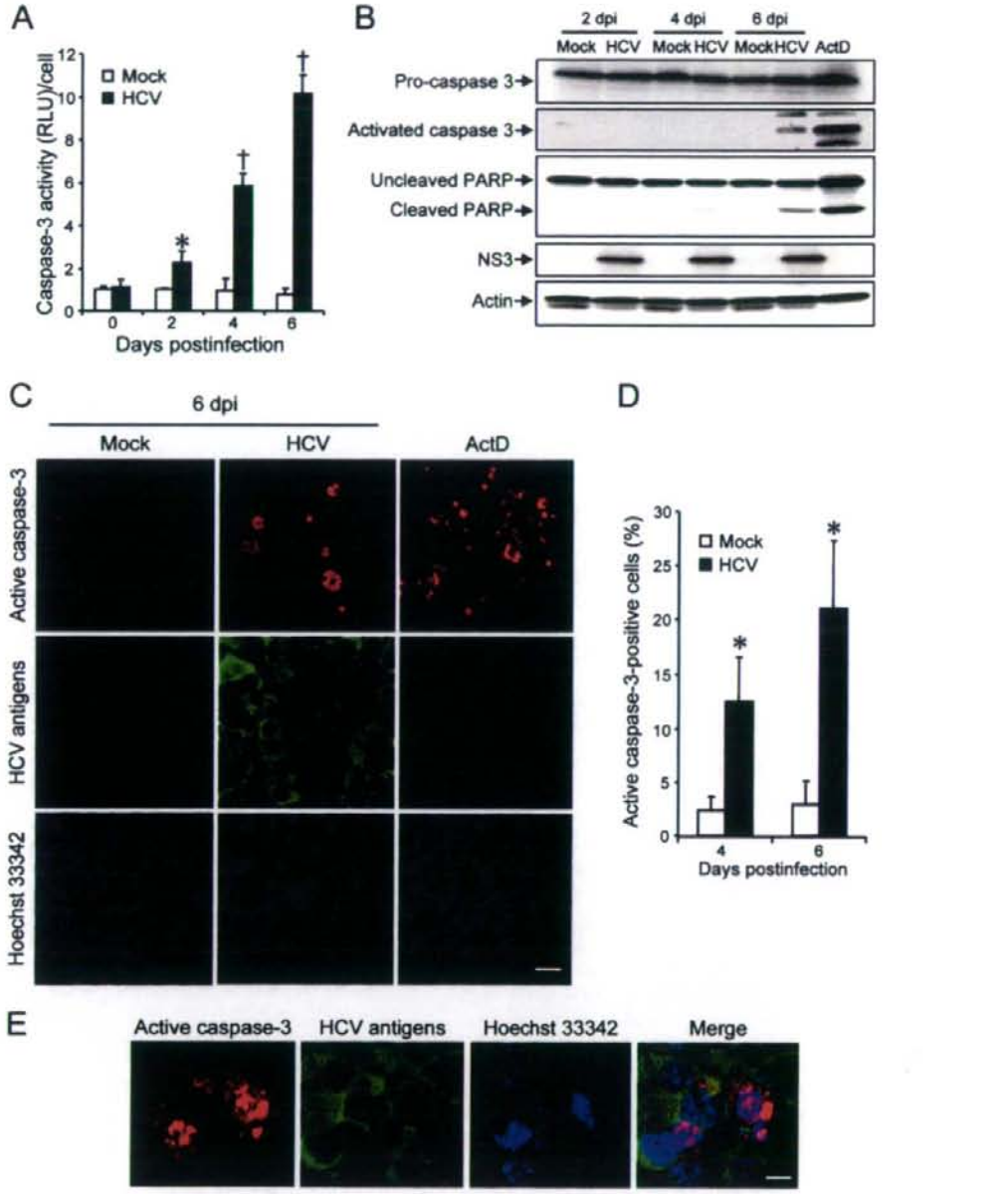

FIG. 2. HCV infection activates caspase 3 in Huh7.5 cells. (A) Caspase 3 activities in cells infected with HCV and mock-infected controls. The caspase 3 activity of the control cells at day 0 postinfection was arbitrarily expressed as 1.0. *, $P < 0.05$; †, $P < 0.01$ (compared with the control). Data represent means ± standard deviations (SD) of three independent experiments. (B) Immunoblot analysis to detect the activated form of caspase 3 (~17 kDa) and cleavage product of PARP (~85 kDa) in HCV-infected cells and the mock-infected control at 2, 4, and 6 days postinfection (dpi). Huh7.5 cells treated with actinomycin D (ActD; 50 ng/ml) for 30 h served as a positive control. Amounts of actin were measured as an internal control to verify an equal amount of sample loading. (C) Huh7.5 cells infected with HCV or mock infected were subjected to indirect immunofluorescence analysis at 6 dpi. Cells treated with ActD (50 ng/ml) for 30 h served as a positive control. After fixation and permeabilization, the cells were incubated with anti-active caspase 3 rabbit polyclonal antibody followed by Cy3-labeled donkey anti-rabbit IgG (top) and with an HCV-infected patient's serum followed by FITC-labeled goat anti-human IgG (middle). The cells were then stained with Hoechst 33342 for the nuclei (bottom). Scale bar, 20 μm. (D) Quantification of active caspase 3-expressing cells. The percentages of cells expressing active caspase 3 were determined for HCV-infected cultures and mock-infected controls. Data represent means ± SD of three independent experiments. *, $P < 0.05$, compared with the control. (E) Nuclear translocation of active caspase 3 in HCV-infected cells. Subcellular localization of active caspase 3 in HCV-infected cells was examined by indirect immunofluorescence analysis at 6 days postinfection as described in the legend for panel C. Scale bar, 5 μm.

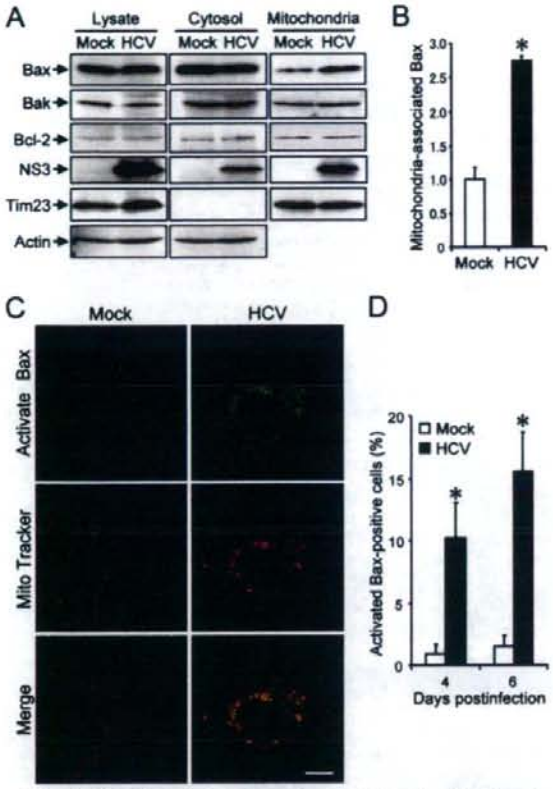

FIG. 3. HCV infection induces Bax activation in Huh7.5 cells. (A) Accumulation of Bax on the mitochondria in HCV-infected Huh7.5 cells. Cytosolic and mitochondrial fractions as well as whole-cell lysates were prepared from HCV-infected cells and the mock-infected control at 6 days postinfection and analyzed by immunoblotting using antibodies against Bax, Bak, Bcl-2, NS3, Tim23, and actin. Amounts of Tim23, a mitochondrion-specific protein, were measured to verify equal amounts of mitochondrial fractions. Amounts of actin were measured to verify equal amounts of whole-cell lysates and cytosolic fractions. (B) The intensities of the bands of mitochondrion-associated Bax in HCV-infected cells and the mock-infected control were quantified. The intensity of the mock-infected control was arbitrarily expressed as 1.0. Data represent means ± standard deviations (SD) of three independent experiments. *, $P < 0.01$, compared with the control. (C) Conformational change of Bax in HCV-infected cells. Huh7.5 cells infected with HCV and the mock-infected control were subjected to indirect immunofluorescence analysis at 6 days postinfection. After incubation with MitoTracker (middle row), the cells were incubated with an antibody specific for the N terminus of Bax (NT antibody), followed by Alexa Fluor 488-labeled goat anti-rabbit IgG (top row). Merged images are shown on the bottom. Scale bar, 10 μm. (D) Quantification of activated Bax-positive cells. The percentages of cells expressing activated Bax were determined for HCV-infected cultures and the mock-infected control. Data represent means ± SD of three independent experiments. *, $P < 0.01$, compared with the control.

HCV antigens. This observation implies the possibility that an indirect effect(s) of HCV infection, in addition to a direct effect of an HCV protein, as observed for NS3/4A (43), is involved in mitochondrial swelling and/or aggregation.

Electron microscopic analysis also demonstrated swelling and structural alterations of mitochondria in HCV-infected cells, whereas mitochondria remained intact in the mock-infected control (Fig. 5C). This result suggests a detrimental effect of HCV infection on the volume homeostasis and morphology of mitochondria and is consistent with previous observations that liver tissues from HCV-infected patients showed morphological changes in mitochondria (3).

Mitochondrial swelling and the morphological change of mitochondrial cristae are associated with cytochrome *c* release (27, 54). We then examined the effect of HCV infection on cytochrome *c* release in Huh7.5 cells. The result clearly demonstrated cytochrome *c* release from the mitochondria to the cytoplasm in HCV-infected cells but not in the mock-infected control (Fig. 6A). The release of cytochrome *c* from mitochondria is known to induce activation of caspase 9 (31). We then analyzed caspase 9 activities in the cells. As shown in Fig. 6B, caspase 9 activities in HCV-infected cells increased to levels that were ca. five times higher than that in the control cells at 4 and 6 days postinfection.

HCV infection induces a marginal degree of caspase 8 activation. In addition to the mitochondrial death (intrinsic) pathway described above, the extrinsic cell death pathway, which is initiated by the TNF family members and mediated by activated caspase 8 (31, 62), is also the focus of attention in the study of apoptosis. Therefore, we examined caspase 8 activities in HCV-infected cells and the mock-infected control. As shown in Fig. 6C, caspase 8 activities in HCV-infected cells increased to a level that was ca. two times higher than that in the control cells at 4 and 6 days postinfection. This increase was much smaller than that observed for caspase 9 activation (Fig. 6B).

HCV infection induces increased production of mitochondrial reactive oxygen species (ROS). The production of ROS, such as superoxide, by mitochondria is the major cause of cellular oxidative stress (8), and a possible link between ROS production and Bax activation has been reported (18, 42). Therefore, we next examined the mitochondrial ROS production in HCV- and mock-infected cells by using MitoSOX, a fluorescent probe specific for superoxide that selectively accumulates in the mitochondrial compartment. As shown in Fig. 7A and B, approximately 25% of HCV-infected cells displayed a much higher signal than did the mock-infected control. This result suggests that oxidative stress is induced by HCV infection.

HCV infection does not induce ER stress. It is well known that HCV nonstructural proteins form the replication complex on the endoplasmic reticulum (ER) membrane (4, 19, 39, 46). It was recently reported that HCV infection (55) as well as the transfection of the full-length HCV replicon (17) and the expression of the entire HCV polyprotein (14) induced an ER stress response. Therefore, we tested whether HCV infection in our system induces ER stress. We adopted increased expression of GRP78 and GRP94 as indicators of ER stress (34) and, as a positive control, used tunicamycin to induce ER stress (20, 25). As had been expected, the expression levels of GRP78 and GRP94 were markedly increased in Huh7.5 cells when cells were treated with tunicamycin for 48 h (Fig. 8, right). On the other hand, HCV infection did not alter expression levels of GRP78 or GRP94 at 2, 4, or 6 days postinfection compared

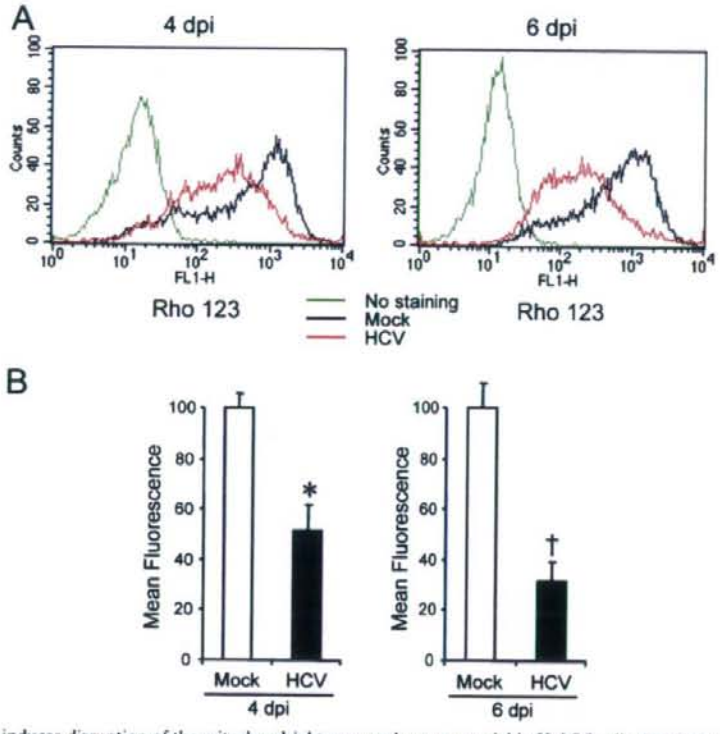

FIG. 4. HCV infection induces disruption of the mitochondrial transmembrane potential in Huh7.5 cells. (A) Huh7.5 cells infected with HCV and the mock-infected control were stained with Rho123 and subjected to flow cytometric analysis to measure the mitochondrial transmembrane potential at 4 and 6 days postinfection (dpi). The red and black lines represent Rho123 staining of HCV-infected cells and the mock-infected control, respectively. The green profiles represent staining of the cells with PBS alone. (B) Mean fluorescence intensities of HCV-infected cells and the mock-infected control at 4 and 6 dpi. Data represent means ± standard deviations (SD) of three independent experiments. *, $P < 0.05$; †, $P < 0.01$ (compared with the control).

with those for the mock-infected control (Fig. 8). This result suggests that ER stress, if there is any, is marginal and does not play an important role in HCV-induced apoptosis in Huh7.5 cells.

DISCUSSION

The mitochondrion is an important organelle for cell survival and death and plays a crucial role in regulating apoptosis. An increasing body of evidence suggests that apoptosis occurs in the livers of HCV-infected patients (1, 2, 9) and that HCV-associated apoptosis involves, at least partly, a mitochondrion-mediated pathway (2). In those clinical settings, however, it is not clear whether apoptosis is mediated by host immune responses through the activity of cytotoxic T lymphocytes or whether it is mediated directly by HCV replication and/or protein expression itself. In experimental settings, ectopic expression of HCV core (13, 36), E2 (12), and NS4A (43) has been shown to induce mitochondrion-mediated apoptosis in cultured cells. However, these observations need to be verified in the context of virus replication. The recent development of an efficient HCV infection system in cell culture (37, 66, 71) has allowed us to investigate whether HCV replication directly causes apoptosis. In the present study, we have demonstrated that HCV infection induces Bax-triggered, mitochondrion-mediated, caspase 3-dependent apoptosis, as evidenced by increased accumulation of Bax on mitochondria and its conformational change (Fig. 3), decreased mitochondrial transmembrane potential (Fig. 4), and mitochondrial swelling (Fig. 5), which lead to the release of cytochrome *c* from the mitochondria (Fig. 6A) and subsequent activation of caspase 9 and caspase 3 (Fig. 6B and 2, respectively).

We also observed increased production of mitochondrial superoxide in HCV-infected cells (Fig. 7). This result is consistent with previous observations that expression of the entire HCV polyprotein (47) or HCV replication (60) enhanced production of ROS, including superoxide, through deregulation of mitochondrial calcium homeostasis. ROS, which are produced through the mitochondrial respiratory chain (8), were reported to trigger conformational change, dimerization, and mitochondrial translocation of Bax (18, 42). It is likely, therefore, that activation of Bax in HCV-infected cells is mediated, at least partly, through increased production of ROS in the mitochondria. Kim et al. (29) reported that ROS is a potent activator of c-Jun N-terminal protein kinase, which can phosphorylate Bax, leading to its activation and mitochondrial translocation. In

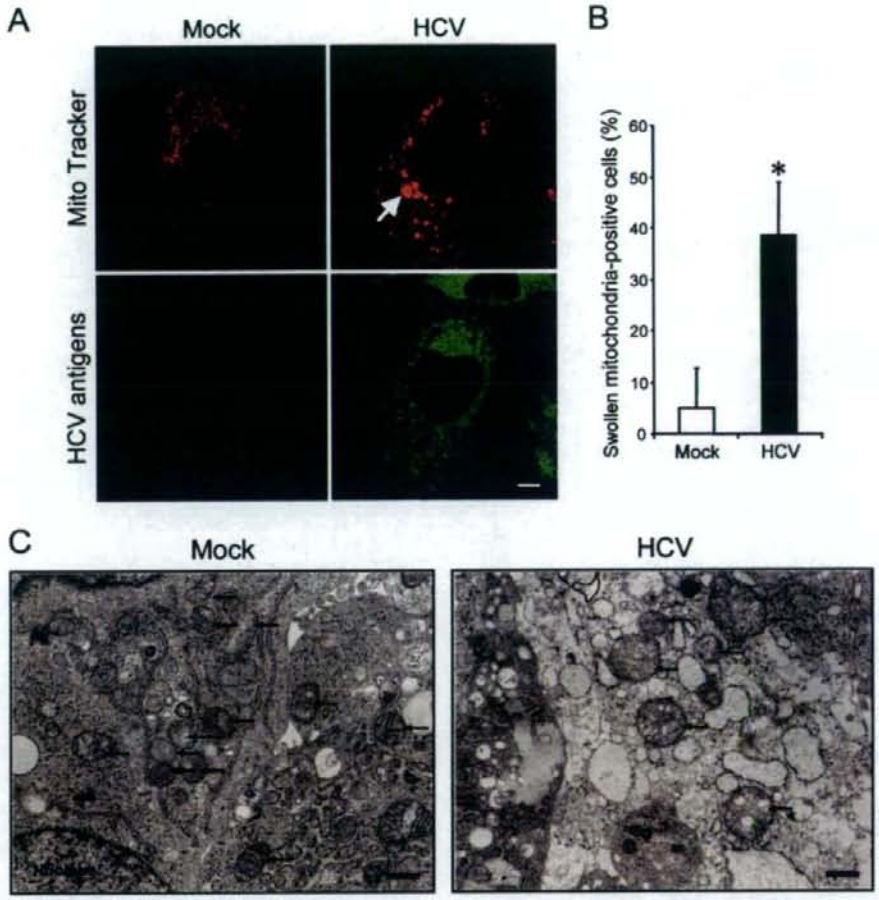

FIG. 5. HCV infection induces mitochondrial morphology changes in Huh7.5 cells. (A) Fluorescence microscopy analysis. Mitochondrial morphologies of HCV-infected cells and the mock-infected control at 6 days postinfection were examined by confocal microscopy. The cells were directly incubated with MitoTracker (upper row) and then stained for HCV antigens by using an HCV-infected patient's serum, followed by FITC-labeled goat anti-human IgG (bottom row). Scale bar, 5 μm. (B) Quantification of swollen mitochondrion-positive cells. The percentages of cells exhibiting swollen and/or aggregated mitochondria were determined for HCV-infected cultures and the mock-infected control. Data represent means ± standard deviations of three independent experiments. *, $P < 0.01$, compared with the control. (C) Electron microscopic analysis. Mitochondrial morphologies of HCV-infected cells and the mock-infected control at 6 days postinfection were examined by electron microscopy. Arrows indicate mitochondria. Scale bar, 1 μm.

this connection, HCV core protein has been shown to play a role in generating mitochondrial ROS (30). It was also reported that HCV core protein bound to the 14-3-3ε protein to dissociate Bax from the Bax/14-3-3ε complex, thereby promoting the Bax translocation to the mitochondria (36).

In addition to the caspase 9 activation that is mediated through the mitochondrial death (intrinsic) pathway, caspase 8 activation was seen in HCV-infected cells, though to a lesser extent (Fig. 6B and C). Caspase 8 is a key component of the extrinsic death pathway initiated by the TNF family members (31, 62). This pathway involves death receptors, such as Fas, TNF receptor, and TNF-related apoptosis-inducing ligand (TRAIL) receptors, which transduce signals to induce apoptosis upon binding to their respective ligands (52). In HCV-infected patients, the Fas-mediated signal pathway is involved in apoptosis of virus-infected hepatocytes (24). It was also reported that HCV (JFH1 strain) infection induced apoptosis through a TRAIL-mediated pathway in LH86 cells (72). On the other hand, a caspase 9-mediated activation of caspase 8, which is considered a cross talk between the intrinsic and the extrinsic death pathways, in certain cell systems was also reported (10, 11, 65). Whether the observed caspase 8 activation in HCV-infected cells was mediated through the extrinsic death pathway initiated by a cytokine(s) produced in the culture or whether it was mediated through the cross talk between the intrinsic and the extrinsic death pathways awaits further investigation. In this connection, activated caspase 8 is known to cleave the proapoptotic protein Bid to generate the Bid

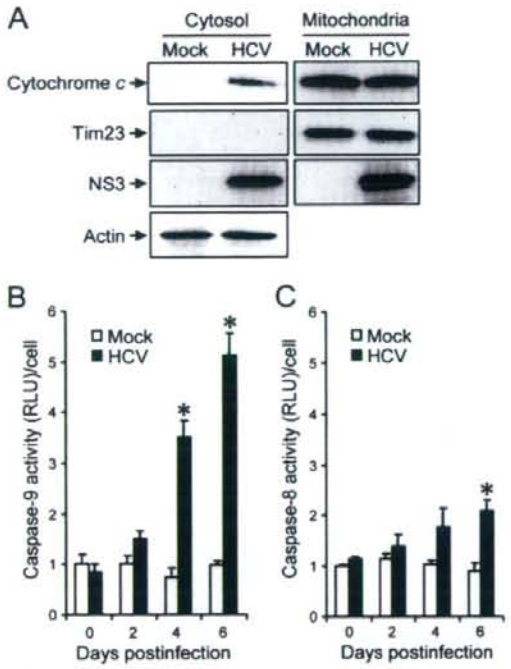

FIG. 6. HCV infection induces cytochrome *c* release and caspase 9 activation in Huh7.5 cells. (A) Cytochrome *c* release. Mitochondrial and cytosolic fractions were prepared from HCV-infected cells and the mock-infected control at 6 days postinfection and analyzed by immunoblotting using antibodies against cytochrome *c*, Tim23, NS3, and actin. Can Get Signal (Toyobo, Osaka, Japan) was used to obtain stronger signals for cytochrome *c*. Amounts of Tim23 and actin were measured to verify equal amounts of mitochondrial and cytosolic fractions, respectively. Also, Tim23 was used to show successful separation of mitochondria. (B) Caspase 9 activation. Caspase 9 activities in cells infected with HCV and mock-infected controls were measured at 0, 2, 4, and 6 days postinfection. The caspase 9 activity of the control cells at day 0 postinfection was arbitrarily expressed as 1.0. Data represent means ± standard deviations (SD) of three independent experiments. *, $P < 0.05$, compared with the control. (C) HCV infection induces a marginal degree of caspase 8 activation. Caspase 8 activities in cells infected with HCV and mock-infected controls were measured at 0, 2, 4, and 6 days postinfection. The caspase 8 activity of the control cells at day 0 postinfection was arbitrarily expressed as 1.0. Data represent means ± SD of three independent experiments. *, $P < 0.05$, compared with the control.

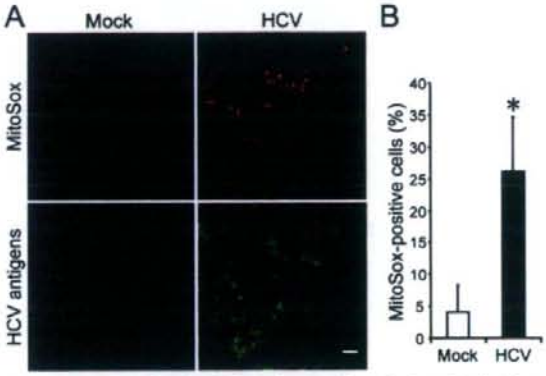

FIG. 7. HCV infection induces increased production of mitochondrial superoxide in Huh7.5 cells. (A) Mitochondrial superoxide production in HCV-infected cells and the mock-infected control was examined at 6 days postinfection. Cells were directly incubated with MitoSOX (upper row) and then stained for HCV antigens by using an HCV-infected patient's serum, followed by FITC-labeled goat anti-human IgG (bottom row). Scale bar, 10 μm. (B) Quantification of MitoSOX-stained cells. The percentages of cells stained with MitoSOX were determined for HCV-infected cultures and the mock-infected control. Data represent means ± standard deviations of three independent experiments. *, $P < 0.05$, compared with the control.

cleavage product truncated Bid (tBid), which facilitates the activation of Bax (63, 68). Under our experimental conditions, however, tBid was barely detected in HCV-infected cells even at 6 days postinfection (data not shown). It is thus likely that caspase 8 activation is marginal and is not the primary cause of Bax activation in our experimental system.

HCV protein expression and HCV RNA replication take place primarily in the ER or an ER-like membranous structure (39, 46). Like other members of the family *Flaviviridae*, such as dengue virus (69), Japanese encephalitis virus (69), West Nile virus (41), and bovine viral diarrhea virus (26), HCV has been reported to induce ER stress in the host cells (5, 14, 17, 55, 60). ER stress is triggered by perturbations in normal ER function, such as the accumulation of unfolded or misfolded proteins in the lumen. On the other hand, in response to ER stress, the unfolded protein response (UPR) is activated to alleviate the ER stress by stimulating protein folding and degradation in the ER as well as by inhibiting protein synthesis (7). The UPR of the host cell is disadvantageous for progeny virus production and may therefore be considered an antiviral host cell response. It was reported that, to counteract the disadvantageous UPR so as to maintain viral protein synthesis, HCV RNA replication suppressed the IRE1-XBP1 pathway, which is responsible for protein degradation upon UPR (59). Also, HCV E2 was shown to inhibit the double-stranded RNA-activated protein kinase-like ER-resident kinase (PERK), which attenuates protein synthesis during ER stress by phosphorylating the alpha subunit of eukaryotic translation initiation factor 2 (45). It is reasonable, therefore, to assume that HCV-infected cells may not necessarily exhibit typical responses to ER stress. In fact, our results revealed that HCV infection in Huh7.5 cells did not enhance

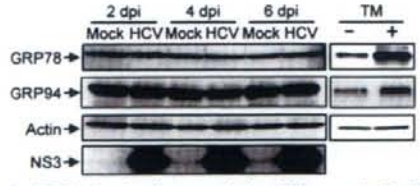

FIG. 8. HCV infection does not induce ER stress in Huh7.5 cells. Huh7.5 cells infected with HCV and mock-infected controls were harvested at 2, 4, and 6 days postinfection (dpi), and the whole-cell lysates were subjected to immunoblot analysis using antibodies against GRP78, GRP94, NS3, and actin. Amounts of actin were measured to verify equal amounts of sample loading. Huh7.5 cells treated with tunicamycin (TM; 5 μg/ml) for 48 h served as a positive control.

expression of GRP78 and GRP94, which are ER stress-induced chaperone proteins (Fig. 8). Our result thus implies the possibility that ER stress is not crucially involved in HCV-induced apoptosis in Huh7.5 cells. Taking advantage of this phenomenon, we could demonstrate that an ER stress-independent, mitochondrion-mediated pathway plays an important role in HCV-induced apoptosis. In this connection, Korenaga et al. (30) reported that HCV core protein increased ROS production in isolated mitochondria, independently of ER stress, by selectively inhibiting electron transport complex I activity.

In this study, we observed that increased ROS production, Bax activation, and caspase 3 activation were detectable in approximately 15% to 25% of HCV antigen-positive Huh7.5cells at 6 days postinfection (Fig. 7B, 3D, and 2D, respectively). On the other hand, >90% of the cells in the cultures were confirmed positive for HCV antigens (Fig. 1B). These results imply the possibility that HCV establishes persistent infection in Huh7.5 cells, with a minor fraction of virus-infected cells beginning to undergo apoptosis after a prolonged period of time. Alternatively, it is possible that Huh7.5 cells, though being derived from a cell line (6), are a mixture of two sublineages, with one sublineage being apoptosis prone and the other apoptosis resistant. To test the latter possibility, further cloning of Huh7.5 cells is now under way in our laboratory.

In conclusion, our present results collectively suggest that HCV infection induces apoptosis through a Bax-triggered, mitochondrion-mediated, caspase 3-dependent pathway.

ACKNOWLEDGMENTS

We are grateful to C. M. Rice (Center for the Study of Hepatitis C, The Rockefeller University) for providing pFL-J6/JFH1 and Huh7.5 cells.

This work was supported in part by grants-in-aid for scientific research from the Ministry of Education, Culture, Sports, Science and Technology (MEXT) and the Ministry of Health, Labor and Welfare, Japan.

This study was carried out as part of the Program of Founding Research Centers for Emerging and Reemerging Infectious Diseases, MEXT, Japan. This study was also part of the 21st Century Center of Excellence Program at Kobe University Graduate School of Medicine.

REFERENCES

1. **Bantel, H., A. Lügering, C. Poremba, N. Lügering, J. Held, W. Domschke, and K. Schulze-Osthoff.** 2001. Caspase activation correlates with the degree of inflammatory liver injury in chronic hepatitis C virus infection. Hepatology **34:**758–767.
2. **Bantel, H., and K. Schulze-Osthoff.** 2003. Apoptosis in hepatitis C virus infection. Cell Death Differ. **10:**S48–S58.
3. **Barbaro, G., G. Di Lorenzo, A. Asti, M. Ribersani, G. Belloni, B. Grisorio, G. Filice, and G. Barbarini.** 1999. Hepatocellular mitochondrial alterations in patients with chronic hepatitis C: ultrastructural and biochemical findings. Am. J. Gastroenterol. **94:**2198–2205.
4. **Bartenschlager, R., M. Frese, and T. Pietschmann.** 2004. Novel insights into hepatitis C virus replication and persistence. Adv. Virus Res. **63:**171–180.
5. **Benali-Furet, N. L., M. Chami, L. Houel, F. De Giorgi, F. Vernejoul, D. Lagorce, L. Buscail, R. Bartenschlager, F. Ichas, R. Rizzuto, and P. Paterlini-Bréchot.** 2005. Hepatitis C virus core triggers apoptosis in liver cells by inducing ER stress and ER calcium depletion. Oncogene **24:**4921–4933.
6. **Blight, K. J., J. A. McKeating, and C. M. Rice.** 2002. Highly permissive cell lines for subgenomic and genomic hepatitis C virus RNA replication. J. Virol. **76:**13001–13014.
7. **Boyce, M., and J. Yuan.** 2006. Cellular response to endoplasmic reticulum stress: a matter of life or death. Cell Death Differ. **13:**363–373.
8. **Brookes, P. S.** 2005. Mitochondrial H^+ leak and ROS generation: an odd couple. Free Radic. Biol. Med. **38:**12–23.
9. **Calabrese, F., P. Pontisso, E. Pettenazzo, L. Benvegnù, A. Vario, L. Chemello, A. Alberti, and M. Valente.** 2000. Liver cell apoptosis in chronic hepatitis C correlates with histological but not biochemical activity or serum HCV-RNA levels. Hepatology **31:**1153–1159.
10. **Camacho-Leal, P., and C. P. Stanners.** 2008. The human carcinoembryonic antigen (CEA) GPI anchor mediates anoikis inhibition by inactivation of the intrinsic death pathway. Oncogene **27:**1545–1553.
11. **Chae, Y. J., H. S. Kim, H. Rhim, B. E. Kim, S. W. Jeong, and I. K. Kim.** 2001. Activation of caspase-8 in 3-deazaadenosine-induced apoptosis of U-937 cells occurs downstream of caspase-3 and caspase-9 without Fas receptor-ligand interaction. Exp. Mol. Med. **4:**284–292.
12. **Chiou, H. L., Y. S. Hsieh, M. R. Hsieh, and T. Y. Chen.** 2006. HCV E2 may induce apoptosis of Huh-7 cells via a mitochondrial-related caspase pathway. Biochem. Biophys. Res. Commun. **345:**453–458.
13. **Chou, A. H., H. F. Tsai, Y. Y. Wu, C. Y. Hu, L. H. Hwang, P. I. Hsu, and P. N. Hsu.** 2005. Hepatitis C virus core protein modulates TRAIL-mediated apoptosis by enhancing Bid cleavage and activation of mitochondria apoptosis signaling pathway. J. Immunol. **174:**2160–2166.
14. **Christen, V., S. Treves, F. H. Duong, and M. H. Heim.** 2007. Activation of endoplasmic reticulum stress response by hepatitis viruses up-regulates protein phosphatase 2A. Hepatology **46:**558–565.
15. **Ciccaglione, A. R., C. Marcantonio, A. Costantino, M. Equestre, and M. Rapicetta.** 2003. Expression of HCV E1 protein in baculovirus-infected cells: effects on cell viability and apoptosis induction. Intervirology **46:**121–126.
16. **Ciccaglione, A. R., C. Marcantonio, E. Tritarelli, M. Equestre, F. Magurano, A. Costantino, L. Nicoletti, and M. Rapicetta.** 2004. The transmembrane domain of hepatitis C virus E1 glycoprotein induces cell death. Virus Res. **104:**1–9.
17. **Ciccaglione, A. R., C. Marcantonio, E. Tritarelli, M. Equestre, F. Vendittelli, A. Costantino, A. Geraci, and M. Rapicetta.** 2007. Activation of the ER stress gene gadd153 by hepatitis C virus sensitizes cells to oxidant injury. Virus Res. **126:**128–138.
18. **D'Alessio, M., M. De Nicola, S. Coppola, G. Gualandi, L. Pugliese, C. Cerella, S. Cristofanon, P. Civitareale, M. R. Ciriolo, A. Bergamaschi, A. Magrini, and L. Ghibelli.** 2005. Oxidative Bax dimerization promotes its translocation to mitochondria independently of apoptosis. FASEB J. **19:**1504–1506.
19. **Egger, D., B. Wölk, R. Gosert, L. Bianchi, H. E. Blum, D. Moradpour, and K. Bienz.** 2002. Expression of hepatitis C virus proteins induces distinct membrane alterations including a candidate viral replication complex. J. Virol. **76:**5974–5984.
20. **Elbein, A. D.** 1987. Inhibitors of the biosynthesis and processing of N-linked oligosaccharide chains. Annu. Rev. Biochem. **56:**497–534.
21. **Erdtmann, L., N. Franck, H. Lerat, J. Le Seyec, D. Gilot, I. Cannie, P. Gripon, U. Hibner, and C. Guguen-Guillouzo.** 2003. The hepatitis C virus NS2 protein is an inhibitor of CIDE-B-induced apoptosis. J. Biol. Chem. **278:**18256–18264.
22. **Griffin, S., D. Clarke, C. McCormick, D. Rowlands, and M. Harris.** 2005. Signal peptide cleavage and internal targeting signals direct the hepatitis C virus p7 protein to distinct intracellular membranes. J. Virol. **79:**15525–15536.
23. **Hidajat, R., M. Nagano-Fujii, L. Deng, M. Tanaka, Y. Takigawa, S. Kitazawa, and H. Hotta.** 2005. Hepatitis C virus NS3 protein interacts with ELKS-δ and ELKS-α, members of a novel protein family involved in intracellular transport and secretory pathways. J. Gen. Virol. **86:**2197–2208.
24. **Jarmay, K., G. Karacsony, Z. Ozsvar, I. Nagy, J. Lonovics, and Z. Schaff.** 2002. Assessment of histological feature in chronic hepatitis C. Hepatogastroenterology **49:**239–243.
25. **Jiang, C. C., L. H. Chen, S. Gillespie, K. A. Kiejda, N. Mhaidat, Y. F. Wang, R. Thorne, X. D. Zhang, and P. Hersey.** 2007. Tunicamycin sensitizes human melanoma cells to tumor necrosis factor-related apoptosis-inducing ligand-induced apoptosis by up-regulation of TRAIL-R2 via the unfolded protein response. Cancer Res. **67:**5880–5888.
26. **Jordan, R., L. Wang, T. M. Graczyk, T. M. Block, and P. R. Romano.** 2002. Replication of a cytopathic strain of bovine viral diarrhea virus activates PERK and induces endoplasmic reticulum stress-mediated apoptosis of MDBK cells. J. Virol. **76:**9588–9599.
27. **Kaasik, A., D. Safiulina, A. Zharkovsky, and V. Veksler.** 2007. Regulation of mitochondrial matrix volume. Am. J. Physiol. Cell Physiol. **292:**C157–C163.
28. **Kamada, S., U. Kikkawa, Y. Tsujimoto, and T. Hunter.** 2005. Nuclear translocation of caspase-3 is dependent on its proteolytic activation and recognition of a substrate-like protein(s). J. Biol. Chem. **280:**857–860.
29. **Kim, B. J., S. W. Ryu, and B. J. Song.** 2006. JNK- and p38 kinase-mediated phosphorylation of Bax leads to its activation and mitochondrial translocation and to apoptosis of human hepatoma HepG2 cells. J. Biol. Chem. **281:**21256–21265.
30. **Korenaga, M., T. Wang, Y. Li, L. A. Showalter, T. Chan, J. Sun, and S. A. Weinman.** 2005. Hepatitis C virus core protein inhibits mitochondrial electron transport and increases reactive oxygen species (ROS) production. J. Biol. Chem. **280:**37481–37488.
31. **Kumar, S.** 2007. Caspase function in programmed cell death. Cell Death Differ. **14:**32–43.
32. **Lalier, L., P. F. Cartron, P. Juin, S. Nedelkina, S. Manon, B. Bechinger, and**